Mimicking the electron transfer chain in Photosystem II with a molecular triad thermodynamically capable of water oxidation

Jackson D. Megiatto Jr.[a], Antaeres Antoniuk-Pablant[a], Benjamin D. Sherman[a], Gerdenis Kodis[a], Miguel Gervaldo[b], Thomas A. Moore[a], Ana L. Moore[a] and Devens Gust[a]

[a]*Center for Bio-Inspired Solar Fuel Production, Department of Chemistry and Biochemistry, Arizona State University, Tempe, AZ 85287.*

[b]*Departamento de Química, Universidad Nacional de Río Cuarto, Agencia Postal 3 (5800), Río Cuarto, Argentina*

Supporting Information

1. Photophysical Section

1.1 - Steady-state spectroscopy

Absorption spectra were measured on a Shimadzu UV2100U UV-vis and/or UV-3101PC UV-vis-NIR spectrometer. Steady-state fluorescence spectra were measured using a Photon Technology International MP-1 spectrometer and corrected for detection system response. Excitation was provided by a 75 W xenon-arc lamp and single grating monochromator. Fluorescence was detected 90^{o} to the excitation beam via a single grating monochromator and an R928 photomultiplier tube having S 20 spectral response and operating in the single photon counting mode.

1.2 - Time-resolved fluorescence

Fluorescence decay measurements were performed by the time-correlated single-photon-counting method. The excitation source was a mode-locked titanium sapphire (Ti:S) laser (Spectra Physics, Millennia-pumped Tsunami) with a 130 fs pulse duration operating at 80 MHz. The laser output was sent through a frequency doubler and pulse selector (Spectra Physics Model 3980) to obtain 370-450 nm pulses at 4 MHz. Fluorescence emission was detected at the magic angle using a double grating monochromator (Jobin Yvon Gemini-180) and a microchannel plate photomultiplier tube (Hamamatsu R3809U-50). The instrument response function was 35-55 ps. The spectrometer was controlled by software based on the LabView programming language and data acquisition was done using a single photon counting card (Becker-Hickl, SPC-830).

1.3 - Transient absorption

For the single kinetics transient absorption measurements a kilohertz pulsed laser source and a pump-probe optical setup were employed. Laser pulses of 100 fs at 800 nm were generated from an amplified, mode-locked titanium sapphire kilohertz laser system (Millennia/Tsunami/Spitfire, Spectra Physics). Part of the laser pulse energy was sent through an optical delay line and focused on to a 2 mm sapphire plate to generate a white light continuum for probe beam. The remainder of the pulse energy was used to pump an optical parametric amplifier (Spectra Physics) to generate excitation pulses, which were modulated using a mechanical chopper. The excitation intensity was adjusted using a continuously variable neutral density filter. The probe beam was sent through a monochromator (SP150, Action Res. Corp.)

and recorded by a diode detector (Model 2032, New Focus Inc.) and box car (SR250, Stanford Research Systems). Instrument response function was ca. 150 fs.

Nanosecond transient absorption measurements were made with excitation from an optical parametric oscillator driven by the third harmonic of a Nd:YAG laser (Ekspla NT342B). The pulse width was ~4-5 ns, and the repetition rate was 10 Hz. The detection portion of the spectrometer (Proteus) was manufactured by Ultrafast Systems. The instrument response function was ca. 4.8 ns.

Data analysis was carried out using locally written software (ASUFIT) developed in a MATLAB environment (Mathworks Inc.). Decay-associated spectra were obtained by fitting the transient absorption or fluorescence change curves over a selected wavelength region simultaneously as described by Eq 1 (parallel kinetic model),

$$\Delta A(\lambda,t) = \sum_{i=1}^{n} A_i(\lambda)\exp(-t/\tau_i) \qquad (1)$$

where $\Delta A(\lambda,t)$ is the observed absorption (or fluorescence) change at a given wavelength at time delay t and n is the number of kinetic components used in the fitting. A plot of $A_i(\lambda)$ versus wavelength is called a decay-associated spectrum (DAS), and represents the amplitude spectrum of the i^{th} kinetic component, which has a lifetime of τ_i.

Evolution-associated difference spectra (EADS) were obtained by global analysis of the transient absorption data using a kinetic model consisting of sequentially interconverting species, e.g. 1→ 2→3→… . The arrows indicate successive mono-exponential decays with increasing time constants, which can be regarded as the lifetimes of each species. Associated with each species is a lifetime and a difference spectrum. Each EADS corresponds in general to a mixture of states and does not portray the spectrum of a pure state or species. This procedure enables us to visualize clearly the evolution of the transient states of the system.

The global analysis procedures described here have been extensively reviewed. (S1) Random errors associated with the reported lifetimes obtained from fluorescence and transient absorption measurements were typically ≤ 5%.

1.4 Photophysical Data

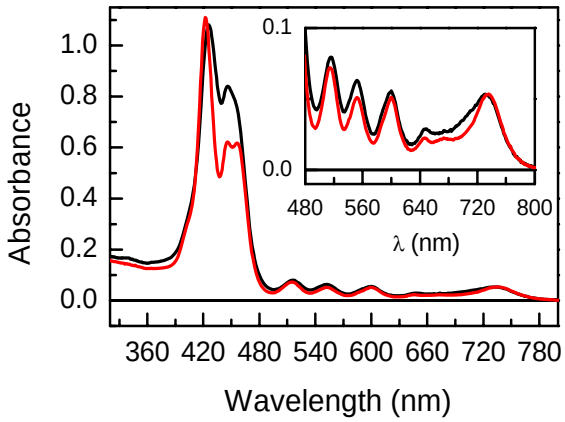

Fig. S1. Ground state absorption spectra in benzonitrile. Bi–PhOH–PF_{10}–TCNP triad **1** (black line) and PF_{10}–TCNP dyad **2** (red line).

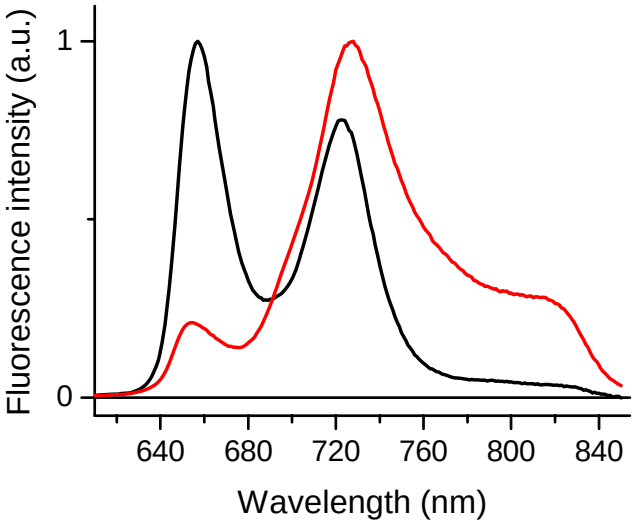

Fig. S2. Fluorescence emission in cyclohexane. PF_{10} model **4** (black line), dyad **2** (red line).

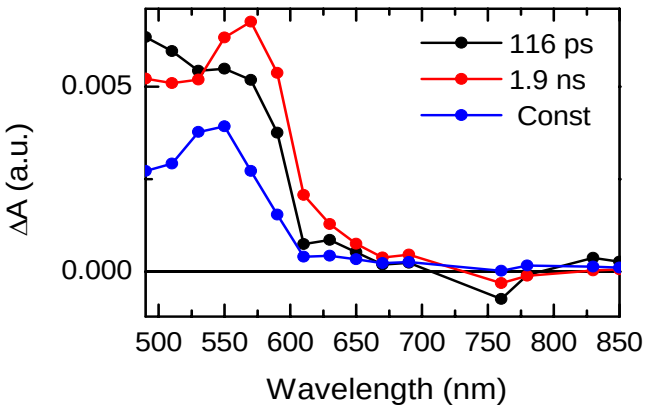

Fig. S3. Transient absorption spectra of TCNP **9** in benzonitrile upon excitation at 740 nm presented in the form of evolution associated difference spectra (EADS). The 116 ps EADS decays into the 1.9 ns EADS and may be attributed to the singlet excited state relaxation of TCNP. This spectral transformation is manifested as a red shift of the induced absorption and stimulated emission. The 1.9 ns EADS shows decay of the relaxed singlet excited state of TCNP into the nondecaying EADS associated with the triplet excited state.

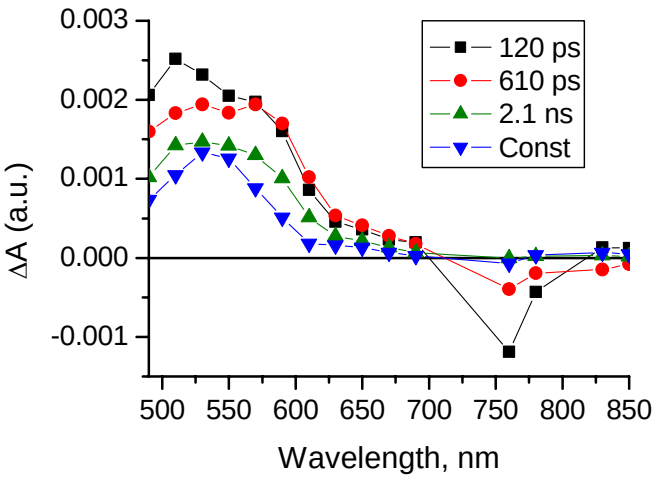

Fig. S4. Transient absorption spectra of triad **1** in benzonitrile upon excitation at 740 nm presented in the form of evolution associated difference spectra (EADS). The 120 ps EADS decays into the 610 ps EADS and is attributed to the singlet excited state relaxation of TCNP. This spectral transformation is manifested as a red shift of the induced absorption and stimulated emission. The 610 ps EADS shows decay of the relaxed singlet excited state of TCNP into the next, 2.1 ns EADS and eventually to the last, nondecaying EADS which is associated with the triplet excited state and BiH^{+}–$PhO^{\bullet}$–PF10–$TCNP^{\bullet-}$ state. The lifetime of the singlet excited state of the TCNP (610 ps) is quenched due to formation of the Bi–PhOH–$PF10^{\bullet+}$–$TCNP^{\bullet-}$ state. As charge shift from the Bi-PhOH moiety to the $PF10^{\bullet+}$ is much faster than 610 ps, it cannot be observed in the transient evolution.

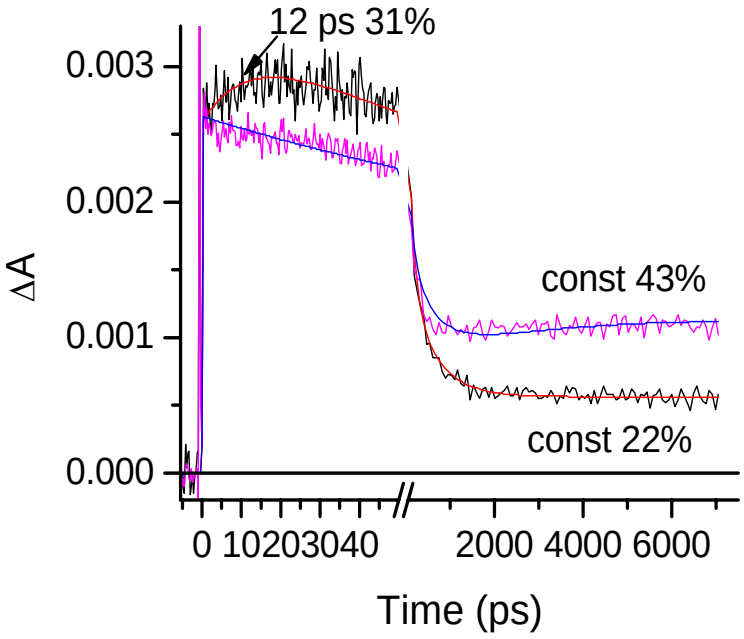

Figure S5. Transient absorption kinetics at 940 nm (induced absorption mostly due to TCNP singlet excited state absorption and radical cation absorption) with excitation at 740 nm of triad **1**

(magenta and blue lines) and dyad **2** in benzonitrile solutions with identical optical densities at 740 nm. Kinetics analysis shows formation of induced absorption due to $TCNP^{\bullet-}$ radical anion with 12 ps, 31% amplitude, in dyad **2**. The nondecaying components correspond only to the TCNP triplet excited state in the dyad case, whereas in the triad the long-lived component has contributions from the porphyrin triplet excited state as well as from the $BiH^{+}-PhO^{\bullet}-PF10-TCNP^{\bullet-}$ final charge separated state. Assuming equivalent formation of triplet excited states in the dyad and triad structures and negligible amount of induced absorption due to $BiH^{+}-PhO^{\bullet}$ at 940 nm, the amplitude of contribution from the final charge separated state in triad **1** can be estimated as 21%. From time resolved emission experiments on dyad **2**, we calculated a quantum yield of 77% for the $PF10^{\bullet+}-TCNP^{\bullet-}$ charge separated state, which corresponds to a 31% amplitude in the kinetic trace. Thus, a rough estimate of the $BiH^{+}-PhO^{\bullet}-PF10-TCNP^{\bullet-}$ quantum yield can be calculated by the Eq 2, which gives x=52%.

$$\frac{31}{21} = \frac{77}{x} \qquad (2)$$

1.5 References

S1. van Stokkum, I. H. M.; Larsen, D. S.; van Grondelle, R. Biochem. Biophys. Acta 2004, 1657, 82-104.

2. Electrochemical and Spectroelectrochemical Studies

All electrochemical and spectroelectrochemical studies were carried out using a CH Instruments 760D potentiostat. For electrochemical experiments, a custom glass cell with Teflon top accommodating a three electrode setup and 1-2 mL of solutions was used. The working electrode was either a platinum or glassy carbon disc electrode as indicated for the particular experiment. The working electrode was combined with a platinum mesh counter electrode and a Ag^{+}/Ag quasi reference. The potential of the Ag^{+}/Ag quasi reference was determined with ferrocenium/ferrocene (Fc^{+}/Fc) as an internal reference, with the potential of the Fc^{+}/Fc couple taken as 0.45 V *vs.* SCE. The compound of interest was dissolved in the indicated solvent, and tetrabutylammonium hexafluorophosphate at a concentration of 100 mM was used as a supporting electrolyte for all experiments. Prior to any experiment, the solution was purged with argon and then run under an argon atmosphere. Spectroelectrochemical experiments were performed with an indium doped tin oxide (ITO) working electrode, with a glass cover slip attached over the conductive face of the ITO with heat-shrink plastic. When immersed in solution, capillary action fills the cavity between the ITO and cover slip and thereby creates a small volume to ensure bulk electrolysis of the solution in the path length of the spectrophotometer in the course of the experiment. The spectroelectrochemical setup was contained in a 1 cm quartz cuvette under a constant Ar flow, and a Shimadzu UV-3101PC spectrophotometer was used for all experiments.

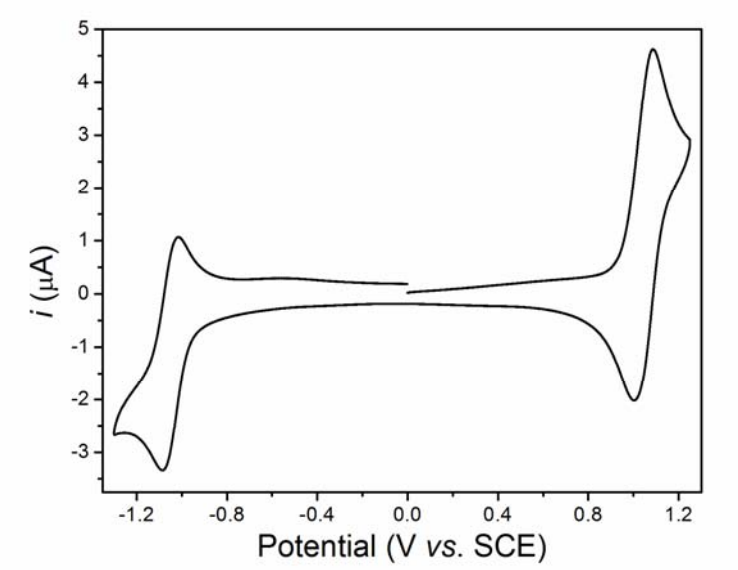

Figure S6. Cyclic Voltammetry of Bi−PhOH−PF_{10} **5**. The voltammogram was taken in dichloromethane with a platinum working electrode and at a scan rate of 100 mV s^{-1}. A reversible oxidation of the complex occurs at 1.04 V *vs.* SCE, corresponding to the Bi−PhOH moiety, and a reversible reduction occurs at -1.05 V *vs.* SCE, corresponding to the PF_{10} moiety.

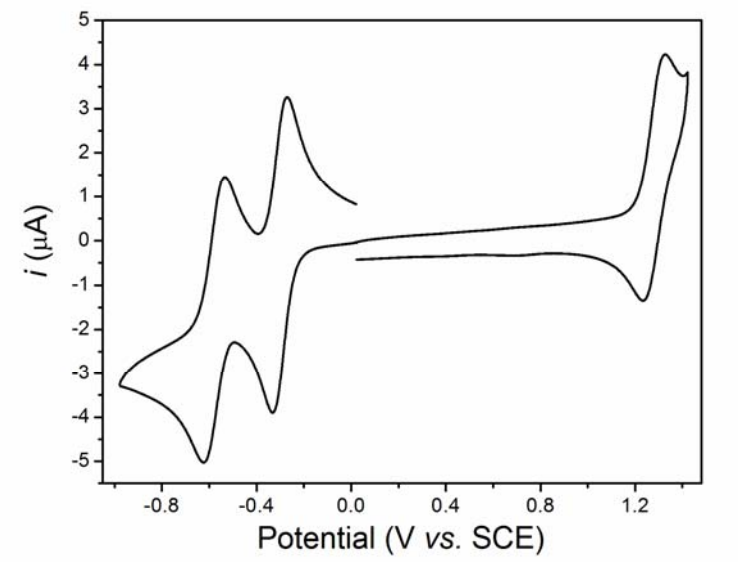

Figure S7. Cyclic Voltammetry of TCNP **9**. This plot is a combination of two scans, one from 0 to -1.0 V, the other from 0 to 1.4 V *vs.* SCE. The cyclic voltammograms were recorded in dichloromethane with a platinum working electrode. Sequential reductions of the TCNP occurred at -0.30 V *vs.* SCE and -0.58 V *vs.* SCE, and an oxidation was observed at 1.28 V *vs.* SCE.

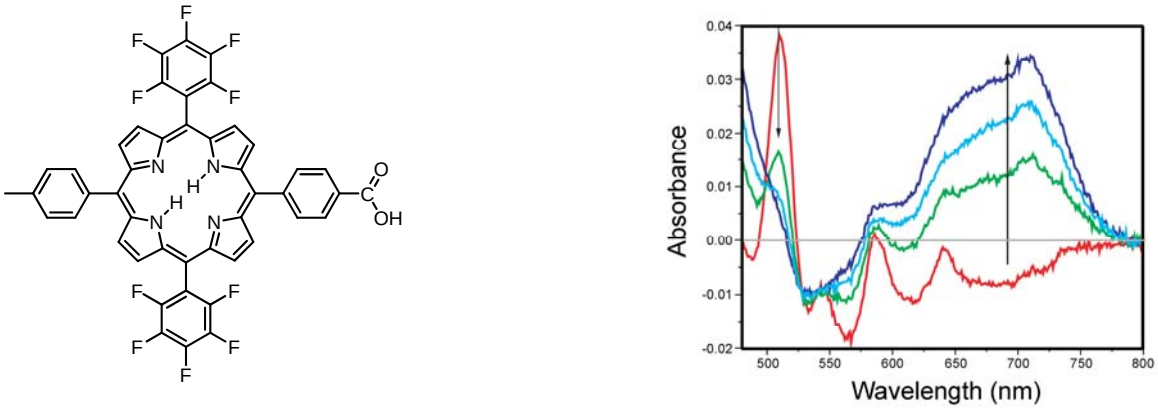

Figure S8. Spectroelectrochemistry of PF_{10} model compound. The structure of the model PF_{10} used is shown on the left. The plot to the right shows the absorbance spectrum of the PF_{10} solution at different times (0 min. (red), 2 min. (green), 4 min. (cyan), and 6 min. (blue)) while poising the solution at 1.30 V *vs.* SCE. The spectrum of the oxidized form of PF_{10} (blue) shows bleaching of the Q bands and a new absorption at around 700 nm. The experiments for this Figure were done in dichloroethane containing $TBAPF_6$ as the supporting electrolyte.

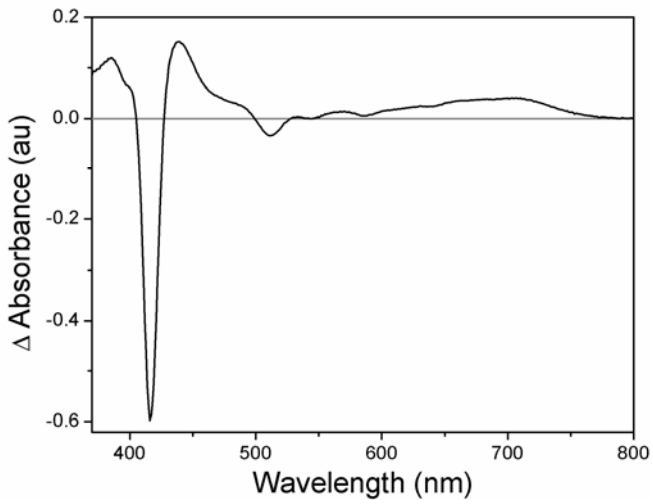

Figure S9. Spectroelectrochemistry of PF_{10} model compound**.** This plot shows the difference in absorption between the absorbance of PF_{10} when poised at 1.30 V *vs.* SCE (singly oxidized) and its absorbance at 0 V *vs.* SCE (neutral state). The spectrum of the oxidized form of PF_{10} shows a bleaching of the Soret band (near 420 nm) and a positive absorption at around 700 nm. The experiments for this Figure were done in dichloroethane containing $TBAPF_6$ as the supporting electrolyte, and the spectra of the neutral and oxidized forms of the porphyrin were taken after poising the working electrode at constant voltage for 6 min.

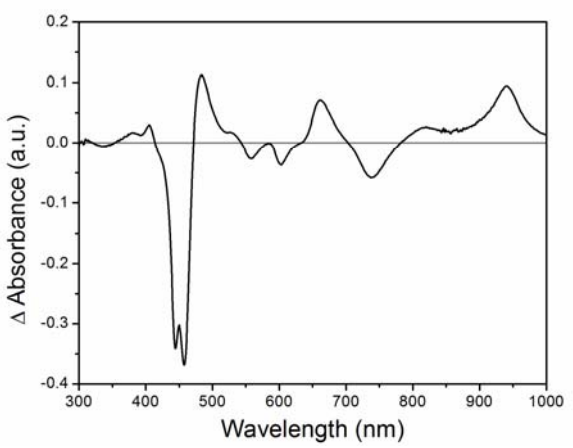

Figure S10. Spectroelectrochemistry of TCNP **9.** This plot shows the difference in absorption between the absorbance of **9** when poised at -0.64 V *vs.* SCE (singly reduced) and its absorbance at -0.04 V *vs.* SCE (neutral state). The spectrum of the reduced form of **9** shows a bleaching of the Soret band (near 450 nm) and induced absorption at 660 nm and 940 nm. The experiments for this Figure were done in benzonitrile and the spectra of the uncharged and reduced forms of the porphyrin were taken after poising the working electrode at constant voltage for 15 min.

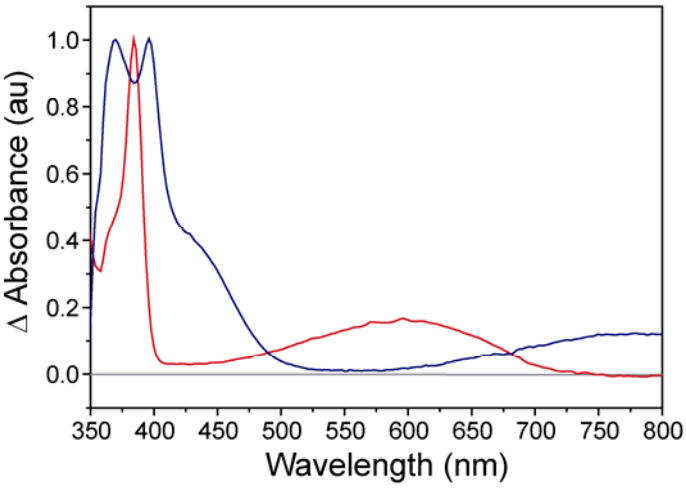

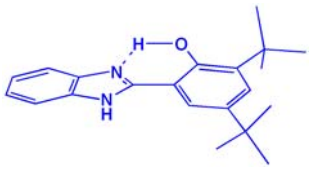

BIP **1**

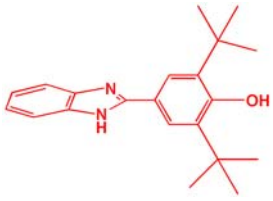

BIP **2**

Figure S11. Spectroelectrochemistry of BIP **1** (blue) and BIP **2** (red). The blue and red traces of the spectrum to the left show the difference in absorption between the oxidized and neutral forms of the corresponding BIP structure. The oxidized form of BIP **1** was generated by poising the working electrode at 1.05 V *vs.* SCE and that of BIP **2** was formed by poising at 0.80 V *vs.* SCE. The spectrum of the oxidized form of BIP **1** shows four positive bands at 370, 400, 445 (shoulder), and 780 nm. For BIP **2,** two bands near 390 and 580 nm can be seen. The experiments for this Figure were done in dichloroethane, and the spectra of the neutral and oxidized forms of the molecules were taken after poising the working electrode at constant voltage for 6 min.

Table 1. Redox potentials (V *vs.* SCE). For reversible processes, the peak separation (ΔE_p) is given in mV.

Compound	Ox(2), (ΔE_p)	Ox(1), (ΔE_p)	Red(1), (ΔE_p)	Red(2), (ΔE_p)	Red(3), (ΔE_p)
BIP-PhOH[a]	-	0.95 (88)	-	-	-
PF_{10}[a]	1.53 (65)	1.29 (65)	-0.96 (84)	-1.37 (82)	-
9[b]	1.51 (irr)	1.28 (93)	-0.30 (63)	-0.58 (92)	-
5[b]	-	1.04 (81)	-1.05 (67)	-	-
2[c]	-	1.23 (irr)	-0.25 (69)	-0.53 (70)	-0.97 (60)
1[d]	-	1.06	-0.27	-0.61	-

[a] These model structures are not included in this work but have been reported in previous studies with a related system (Moore, G. F., *et al. J. Am. Chem. Soc.* 2008, 130: 10466-10467).[b] Cyclic voltammetry done in dichloromethane solution with a platinum working electrode.[c] Cyclic voltammetry done in actetonitrile solution with a glassy carbon working electrode.[d] Values obtained by differential pulse voltammetry in benzonitrile with a glassy carbon working electrode.

3. Synthetic Section

3.1 – Materials

All chemicals were purchased from Aldrich, Alfa Aesar, and Acros and were used without further purification. Solvents were obtained from EM Science and were used as received unless otherwise noted. Thin layer chromatography (TLC) was performed with silica gel coated glass plates from Analtech. Column chromatography was carried out using Silicycle silica gel 60 with 230-400 mesh.

3.2 – Spectroscopic Measurements

The ^{1}H-NMR spectra were recorded on a Varian spectrometer at 400 MHz or 500 MHz. NMR samples were prepared in deuteriosolvents with tetramethylsilane as an internal reference using a Wilmad 528-PP 5 mm NMR tube. Deuterated chloroform was distilled from CaH. Mass spectra were obtained with a matrix-assisted laser desorption/ionization time-of-flight spectrometer (MALDI-TOF), using (1E, 3E)-1,4-diphenylbuta-1,3-diene (DPB), cyano-4-hydroxycinnamic acid (CCA) or terthiophene as a matrix. The reported mass is of the most abundant isotopic ratio observed. To facilitate comparison, calculated values of the expected most abundant isotopic ratio are listed after the experimental result.

3.3. – Synthesis of Building Blocks, Synthetic Intermediates and Their Spectroscopic Characterization

Overview of Synthetic Strategy:

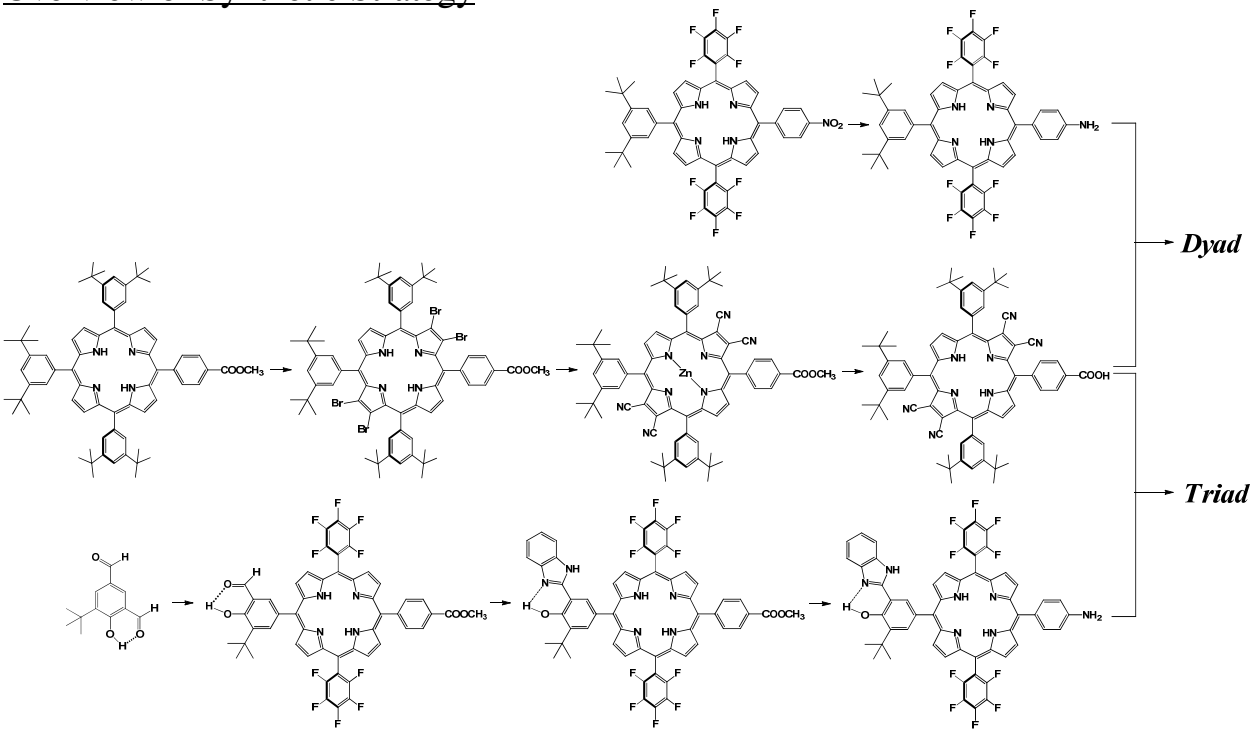

Synthesis of 5-formyl-3-tert-butyl-2-hydroxybenzaldehyde **3**:[S2]

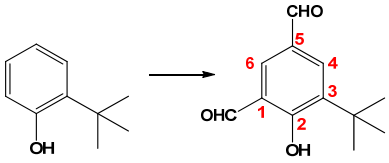

A solution of commercially available 2-tert-butylphenol (6.00 g, 40 mmol, 1 equiv.), hexamethylenetetramine (14.00 g, 100 mmol, 2.5 equiv.) and trifluoroacetic acid (40 mL) was heated at reflux for 12 h. The reaction was quenched while hot with a 33% (v/v) aqueous H_2SO_4 solution (20 mL) and the resulting mixture was allowed to cool to room temperature with stirring. The crude product was extracted with diethyl ether (3 × 50 mL), and the extract was neutralized with a saturated aqueous solution of sodium bicarbonate (2 × 100 mL) and finally washed with water (3 × 100 mL). The organic phase was dried over sodium sulfate, filtered through paper and concentrated under reduced pressure. Final purification was achieved by column chromatography (SiO_2), using hexanes/EtOAc (9:1, v/v) as eluent to afford the title compound as a light yellow solid in 55% yield (4.53 g). ^{1}H NMR (400 MHz, $CDCl_3$, δ ppm): 12.37 (s, 1H, O<u>H</u>); 9.96 (s, 1H, C<u>H</u>O); 9.89 (s, 1H, C<u>H</u>O); 8.03 (d, J = 2.0 Hz, 1H, Ar<u>H</u>$_6$); 7.96 (d, J = 2.0 Hz, 1H, Ar<u>H</u>$_4$); 1.42 (s, 9H, Bu$_t$).

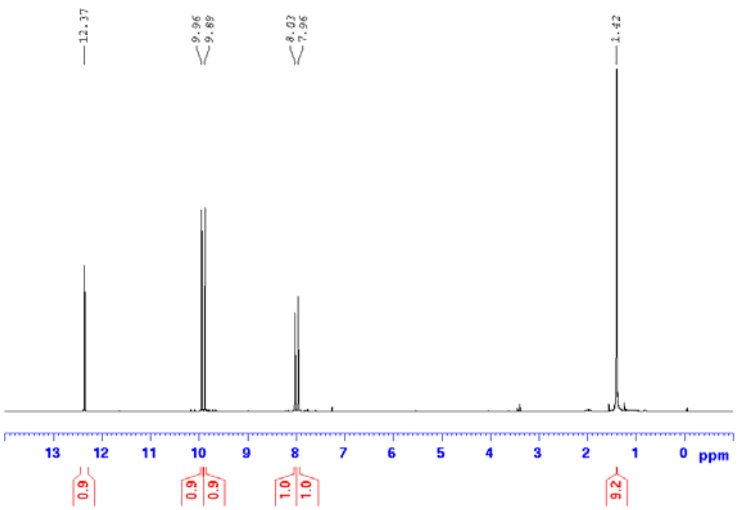

Figure S12. ^{1}H NMR spectrum of compound **3**, 400 MHz, $CDCl_3$, 25^{o}C.

Synthesis of 5-(pentafluorophenyl)dipyrromethane (S2):

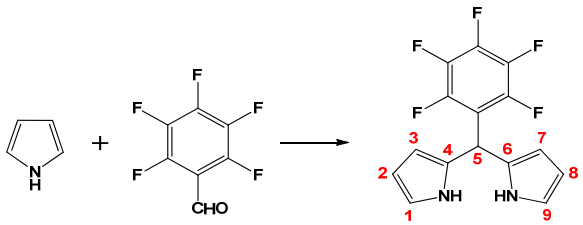

A solution of pentafluorobenzaldehyde (2.0 mL, 16.2 mmol) in freshly distilled pyrrole (50 mL, 720 mmol) was degassed with a stream of argon for 10 min before adding trifluoroacetic acid (120 µL, 1.62 mmol). The mixture was stirred for 30 min at room temperature, diluted with CH_2Cl_2 (400 mL), and then washed with 0.1M NaOH (400 mL). The organic phase was washed with water (400 mL) and dried over Na_2SO_4. Evaporation of the solvent at reduced pressure gave a brown oil. Unreacted pyrrole was removed under high vacuum at room temp, yielding a tacky solid that was purified by flash chromatography on a column of silica using a mixture of hexanes:ethyl acetate:triethylamine (80:20:1) as the eluent. The product was recrystallized from dichloromethane/hexanes to yield 3.29 g of 5-(pentafluorophenyl)dipyrromethane as a white powder in 65% yield (3.28 g). ^{1}H NMR (400 MHz, $CDCl_3$, δ ppm): 8.11 (2H, brs, N$\underline{H}$), 6.73 (2H, m, C$\underline{H}_1$ and C$\underline{H}_9$), 6.16 (2H, m, C$\underline{H}_2$ and C$\underline{H}_8$), 6.02 (2H, brs, C$\underline{H}_3$ and C$\underline{H}_7$), 5.89 (1H, brs, C$\underline{H}_5$), 5.29 (residual solvent C$\underline{H}_2Cl_2$), 1.56 (residual water in the deuterated solvent).

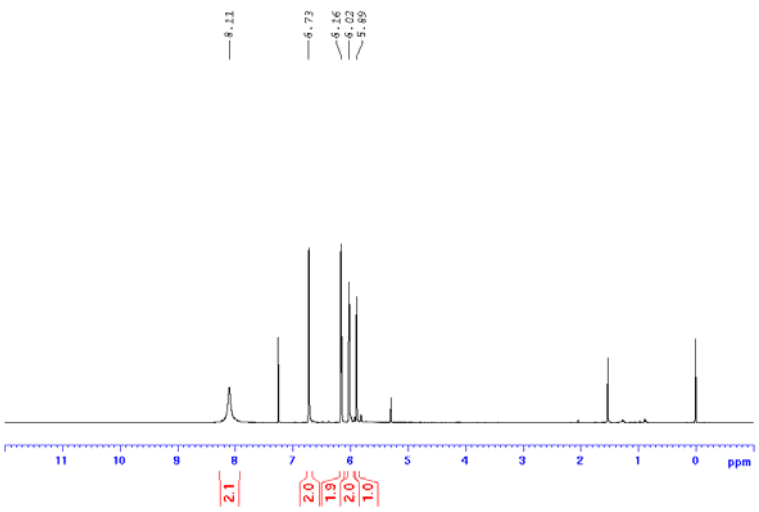

Figure S13. ^{1}H NMR spectrum of 5-(pentafluorophenyl)dipyrromethane, 400 MHz, $CDCl_3$, 25^{o}C.

Synthesis of 5,15-bis(2,3,4,5,6-pentafluorophenyl)-10-(4-carbomethoxyphenyl)-20-(3-formyl-4-hydroxy-5-*tert*-butylpheynyl)porphyrin **4**:

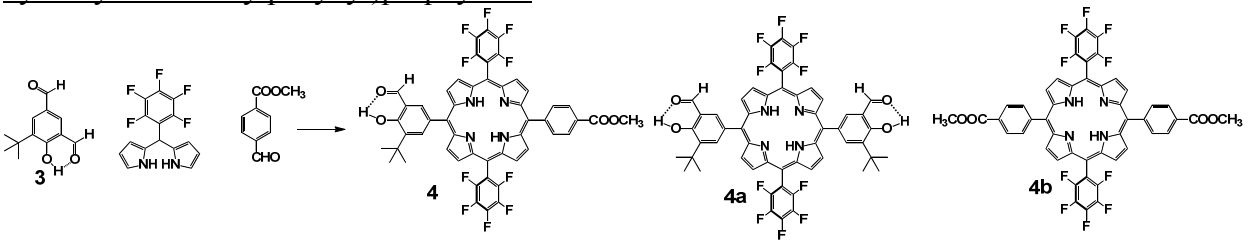

Compound **3** (0.265 g, 1.28 mmol), pentafluorophenyl-dipyrromethane (0.800 g, 2.56 mmol) and carboxymethyl benzoate (0.211 g, 1.56 mmol) were dissolved in 325 mL of chloroform containing 2.45 mL (0.75 %, v/v) of ethanol under a nitrogen atmosphere, followed by addition of boron-trifluoride etherate (BF_3OEt_2) (0.142 g, 0.125 mL, 1.00 mmol) and the reaction mixture was stirred for one hour at room temperature. The resulting dark red porphyrogenic mixture was oxidized with 2,3-dichloro-5,6-dicyano-1,4-benzoquinone (DDQ) (0.732 g, 3.25 mmol) for 12 h at room temperature, yielding a black crude mixture. Filtration through a silica pad to remove tar and polymeric byproducts, followed by concentration under reduced pressure afforded a deep purple reddish solid. Purification through column chromatography (SiO_2, hexanes/dichloromethane as eluent) yielded three porphyrin fractions (23% total porphyrin yield). The first porphyrin fraction corresponded to compound **4a** (0.178 g, 7% yield) followed by target porphyrin **4** (0.268 g, 11% yield) and compound **4b** (0.116 g, 5% yield). A small amount of the target porphyrin **4** was recrystallized from slow evaporation of an acetonitrile solution of **4** in order to afford an analytical sample for spectroscopic characterization.

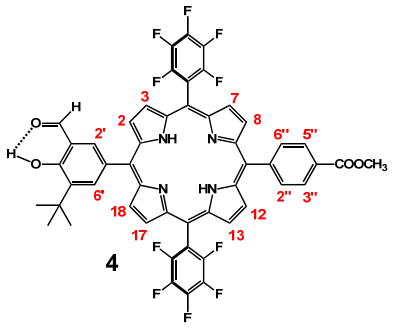

^{1}H NMR (400 MHz, $CDCl_3$, δ ppm): 12.20 (1H, s, OH), 10.12 (1H, s, CHO), 8.93 (2H, d, J = 5.0 Hz, H_8 and H_{12}), 8.67 (2H, d, J = 5.0 Hz, H_2 and H_{18}), 8.79 (4H, t, H_3, H_7, H_{13} and H_{17}), 8.45 (2H, d, J = 8.3 Hz, $H_{3''}$ and $H_{5''}$), 8.39 (1H, d, J = 2.0 Hz, $H_{2'}$), 8.28 (2H, brt, $H_{2''}$ and $H_{6''}$), 8.20 (1H, d, J = 2.0 Hz, $H_{6'}$), 4.12 (3H, s, $COOCH_3$), 1.58 (9H, s, $C(CH_3)_3$), - 2.85 (2H, s, NH).

MALDI-TOF: (positive mode, 1,4-diphenylbutadiene as matrix) 952.46 $(M)^+$, calculated 952.21 for $C_{51}H_{30}F_{10}N_4O_4$.

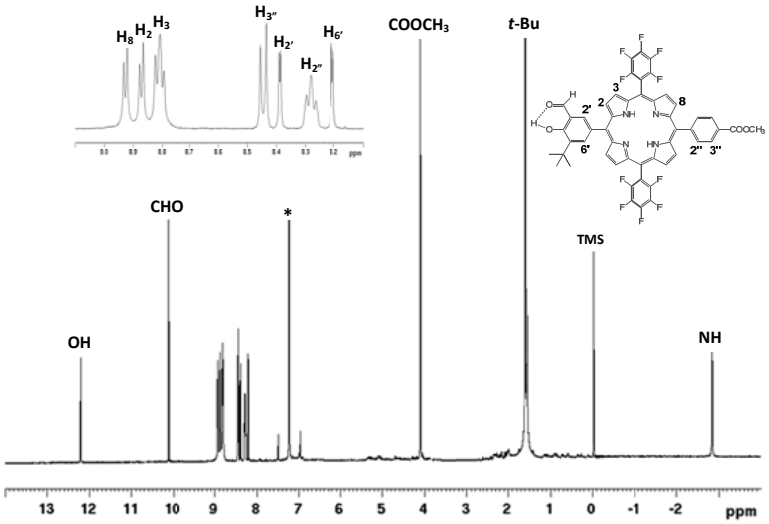

Figure S14. ^{1}H NMR spectrum of porphyrin **4**, 500 MHz, $CDCl_3$, 25°C.

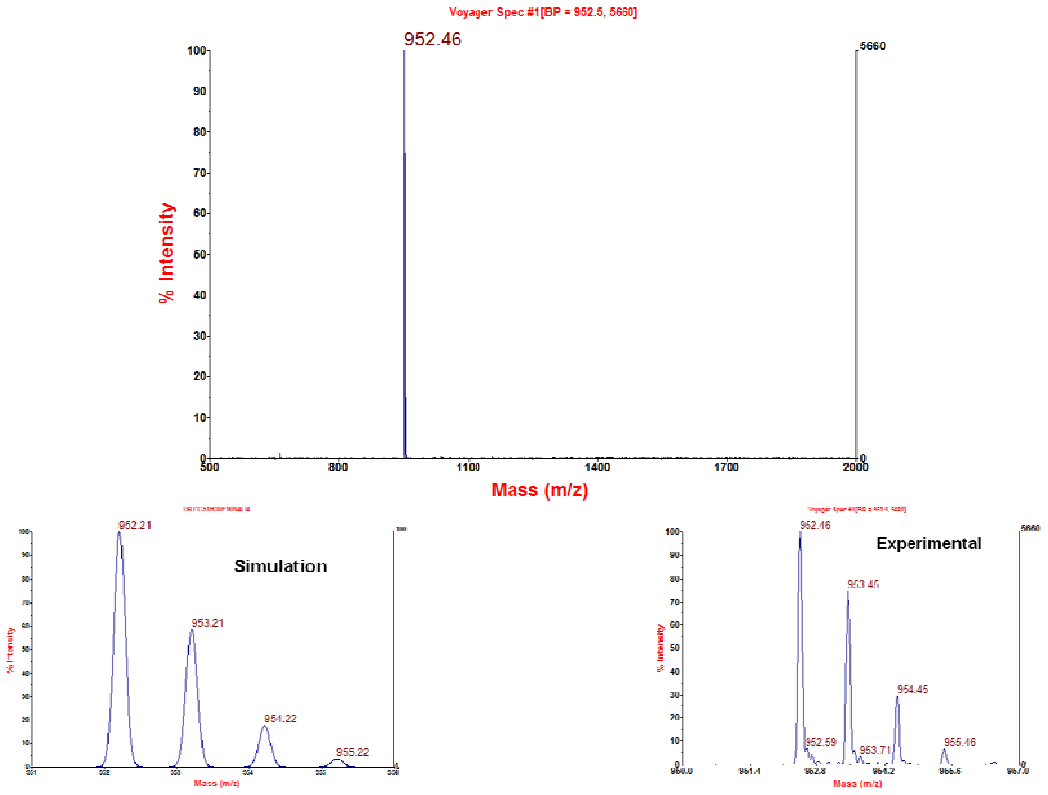

Figure S15. MALDI-TOF spectrum (positive mode, 1,4-diphenylbutadiene as matrix) of compound **4** (top and bottom right) and the corresponding isotope simulation (bottom left) expected for $C_{51}H_{30}F_{10}N_4O_4$.

Synthesis of 5,15-*bis*(2,3,4,5,6-pentafluorophenyl)-10-(4-carbomethoxyphenyl)-20-[2'-(3-*tert*-butyl-2"-hydroxyphenyl)benzimidazole]porphyrin **5**:

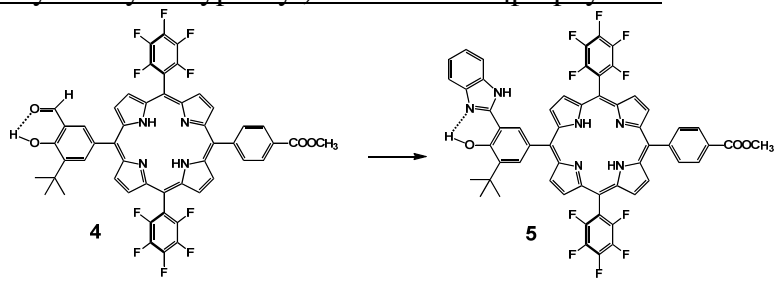

Commercially available 1,2 phenylenediamine (0.0045 g, 0.042 mmol) in nitrobenzene (3 mL) was added drop-wise to a solution of porphyrin **4** (0.040 g, 0.042 mmol) in nitrobenzene (7 mL) and the purple solution was heated at reflux (210 ^{o}C) in a sand-bath for 12 h. After cooling and without any workup, the crude mixture was transferred to a column chromatography (SiO_2 in hexanes) and nitrobenzene was eluted with a mixture of hexanes/dichloromethane (90:10, v/v). The target compound was eluted with a hexanes/dichloromethane (50:50, v/v), which was washed with hexanes (20 mL) to afford **5** as a purple solid in 70% yield (0.031 g). ^{1}H NMR (500 MHz, $(CD_3)_2CO$, δ ppm): 14.57 (s, 1H, OH); 12.42 (s, 1H, NH); 9.25 (m, 6H, pyrrolic protons); 9.10 (d, 2H, J = 4.8 Hz, pyrrolic protons); 8.82 (d, 1H, J = 2.0 Hz, $H_{2'}$); 8.48 (m, 4H, H_2, H_3, H_5 and H_6); 8.38 (d, 1H, J = 2.0 Hz, $H_{6'}$); 7.84 (d, 1H, J = 7.6 Hz, $H_{7''}$); 7.50 (d, 1H, J = 7.6 Hz, $H_{4''}$); 7.30 (m, 2H, $H_{5''}$ and $H_{6''}$); 4.10 (s, 3H, $COOCH_3$); 1.70 (s, 9H, Bu_t); -2.79 (s, 2H, NH). MALDI-TOF (positive mode, 1,4-diphenylbutadiene as matrix) 1041.41 $(M + H)^+$, calculated 1040.25 for $C_{57}H_{34}F_{10}N_6O_3$.

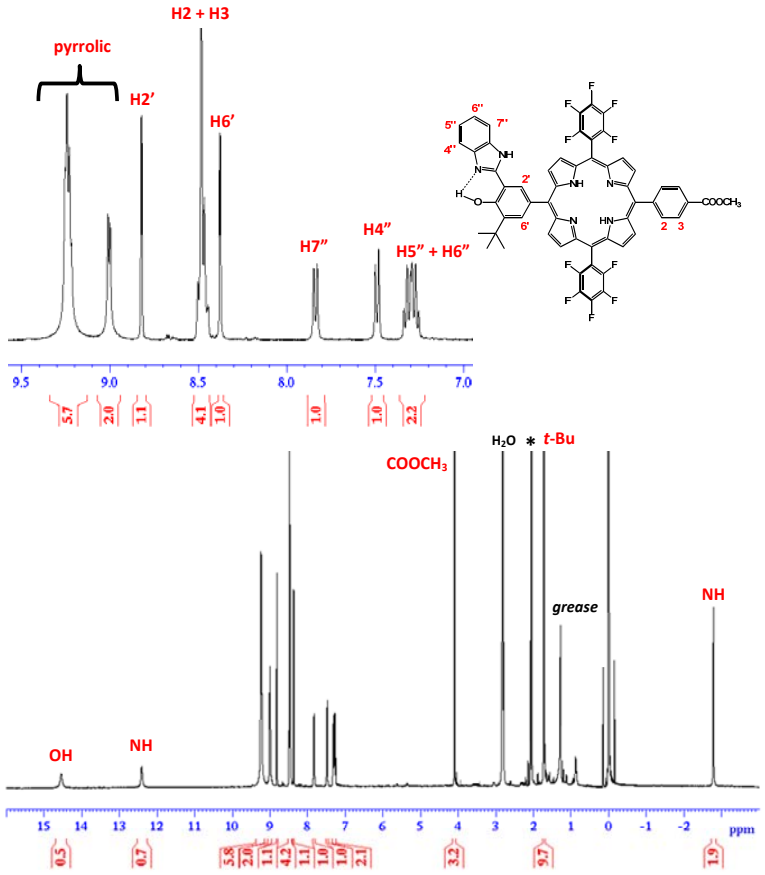

Figure S16. ^{1}H NMR spectrum of porphyrin **5**, 500 MHz, $(CD_3)_2CO$, 25^{o}C.

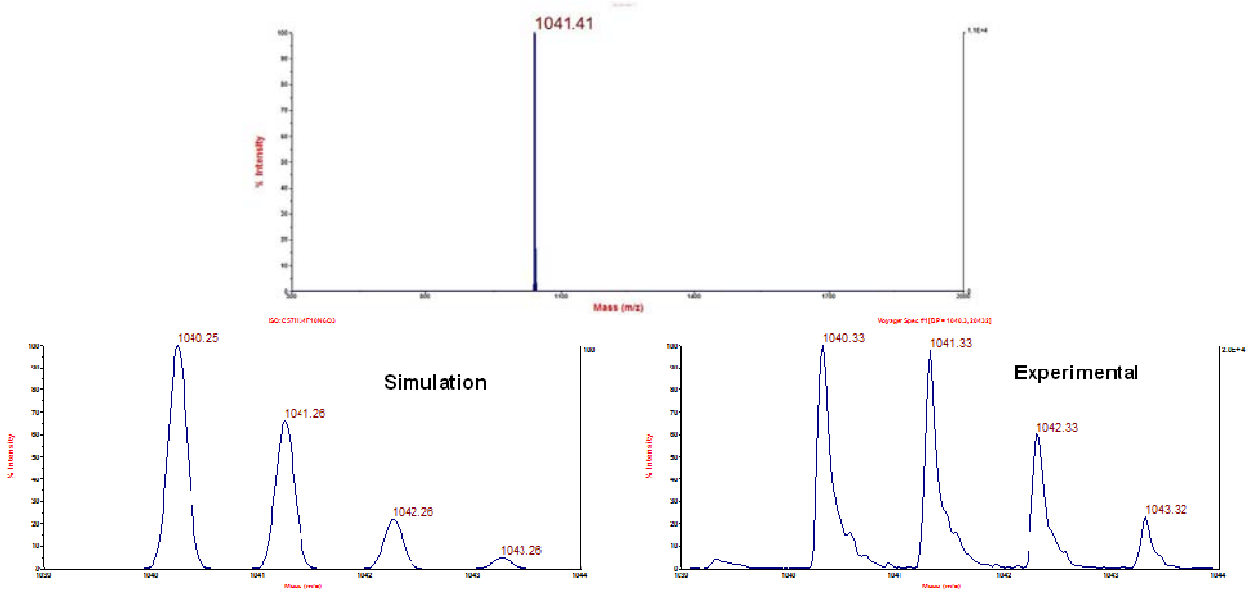

Figure S17. MALDI-TOF spectrum (positive mode, 1,4-diphenylbutadiene as matrix) of porphyrin **5** (top and bottom right) and corresponding isotope simulation (bottom left) expected for $C_{57}H_{34}F_{10}N_6O_3$.

Synthesis of 5,15-*bis*(2,3,4,5,6-pentafluorophenyl)-10-(4-carboxyphenyl)-20-[2'-(3-*tert*-butyl-2"-hydroxyphenyl)benzimidazole]porphyrin **6**:

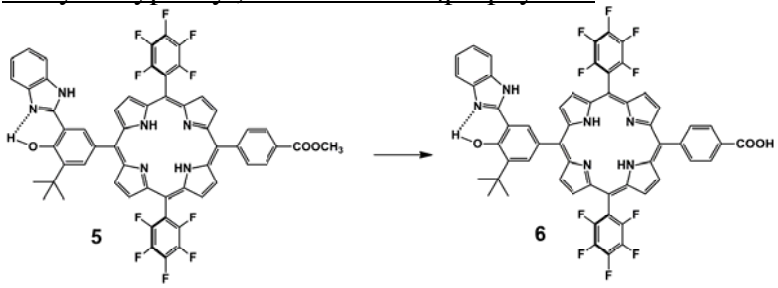

Porphyrin **5** (0.042 g, 0.04 mmol) was dissolved in trifluoroacetic acid (10 mL) followed by addition of 20 mL of concentrated HCl. The green mixture was stirred at 90°C for 24 h. After cooling, the mixture was taken upon dichloromethane (50 mL), washed with water (50 mL) and then neutralized with a saturated sodium carbonate aqueous solution. The organic phase was dried over sodium sulfate, filtered through paper, and concentrated under reduced pressure. The crude product was purified by flash chromatography (SiO_2) using a mixture of dichloromethane/methanol (9:1, v/v) as eluent to afford 0.041 g (98% yield) of the target porphyrin **6** as a purple solid. MALDI-TOF (positive mode, 1,4-diphenylbutadiene as matrix) 1026.41 $(M)^+$, calculated 1026.20 for $C_{56}H_{32}F_{10}N_6O_3$.

Synthesis of 5,15-*bis*(2,3,4,5,6-pentafluorophenyl)-10-(4-aminophenyl)-20-[2'-(3-*tert*-butyl-2"-hydroxyphenyl)benzimidazole]porphyrin **7** (Curtius Rearrangement):

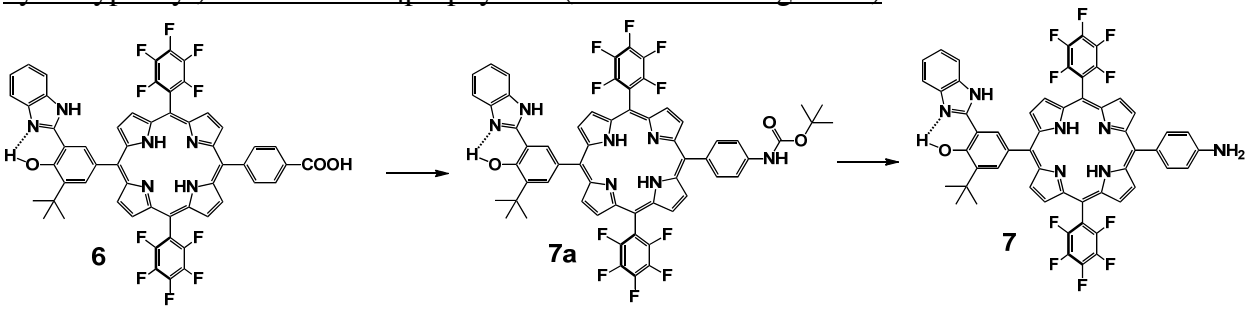

Porphyrin **6** (0.040 g, 0.039 mmol), diphenyl-phosphoryl azide (0.021 g, 0.078 mmol), and triethylamine (20 μL) were dissolved in fresh distilled (from K_2CO_3) *tert*-butanol (10 mL) and heated at 85°C for 24 h. Upon cooling, the reaction mixture was diluted with dichloromethane (50 mL) and then washed with water (3 × 50 mL). The organic phase was dried over sodium sulfate, filtered through paper and concentrated under reduced pressure. Final purification was achieved by column chromatography (SiO_2) using a mixture of hexanes/ethyl acetate (9:1, v/v) as eluent to afford 0.024 g (58 % yield) of the NH-Boc protected porphyrin **7a** as a purple solid. MALDI-TOF (positive mode, 1,4-diphenylbutadiene as matrix) 1097.26 $(M)^+$, calculated 1097.30 for $C_{60}H_{41}F_{10}N_7O_3$. Porphyrin **7a** (0.024 g, 0.022 mmol) was dissolved in 10 mL of trifluoroacetic acid and heated at 90°C for 12 h. The cooled reaction mixture was diluted with dichloromethane (20 mL), washed with water (2 × 50 mL) and then neutralized with a saturated solution of aqueous sodium bicarbonate, followed by washing with water (1 × 50 mL). The organic phase was dried over sodium sulfate, filtered through paper and concentrated under reduced pressure. Final purification was achieved by column chromatography (SiO_2) using dichloromethane as eluent to afford g 0.020 (90% yield) of the amino porphyrin **7** as a purple solid. ^{1}H NMR (500 MHz, $(CD_3)_2CO$, δ ppm): 14.58 (br, 1H, OH); 12.46 (br, 1H, NH); 9.20 (m, 8H, pyrrolic protons); 8.79 (d, 1H, J = 2.0 Hz, $H_{2'}$); 8.38 (d, 1H, J = 2.0 Hz, $H_{6'}$); 8.02 (dbr, 2H, J = 8.0 Hz, $H_{7''}$); 7.89 (d, 1H, J = 7.6 Hz, $H_{4''}$); 7.53 (d, 1H, J = 7.6 Hz, $H_{4''}$); 7.36 (m, 2H, $H_{5''}$ and $H_{6''}$); 7.18 (d, 2H, J = 8.0 Hz, $H_{4''}$); 5.23 (s, 2H, NH_2); 1.72 (s, 9H, Bu_t); -2.70 (d, 2H, NH). MALDI-TOF (positive mode, 1,4-diphenylbutadiene as matrix) 997.53 $(M)^+$, calculated 997.30 for $C_{55}H_{33}F_{10}N_7O$.

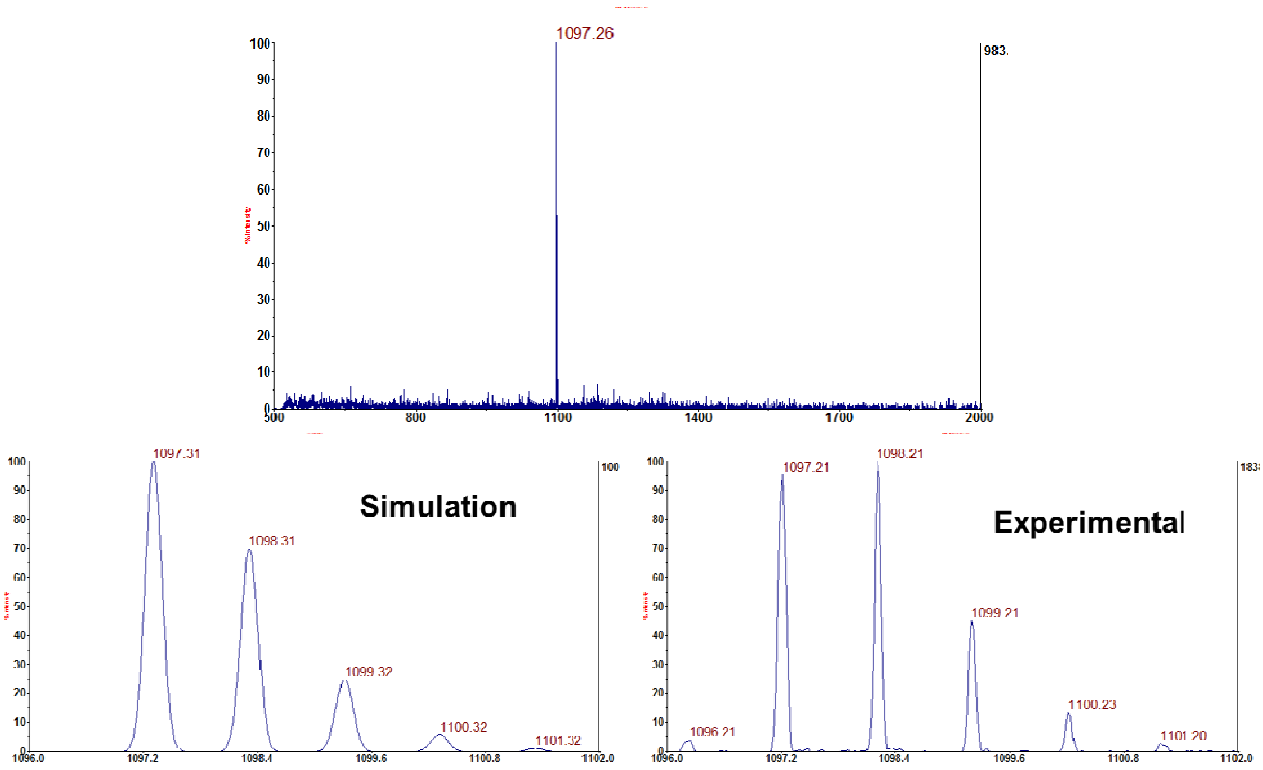

Figure S18. MALDI-TOF spectrum (positive mode, 1,4-diphenylbutadiene as matrix) of porphyrin **7a** (top and bottom right) and corresponding isotope simulation (bottom left) expected for $C_{60}H_{41}F_{10}N_7O_3$.

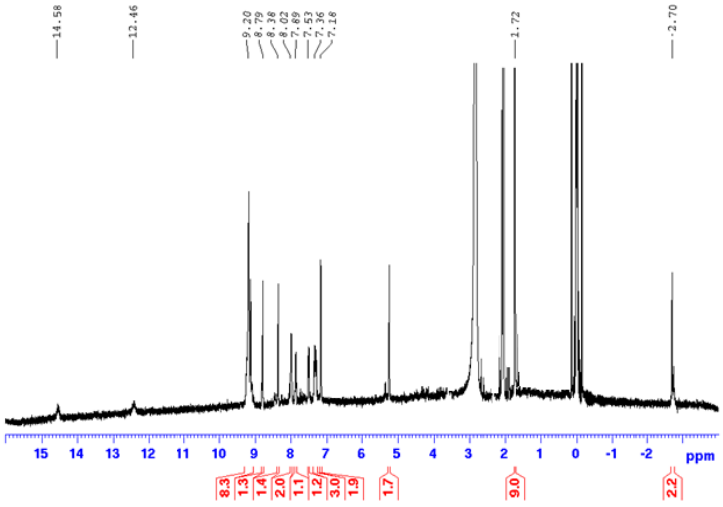

Figure S19. ^{1}H NMR spectrum of porphyrin **7**, 500 MHz, $(CD_3)_2CO$, 25^{o}C.

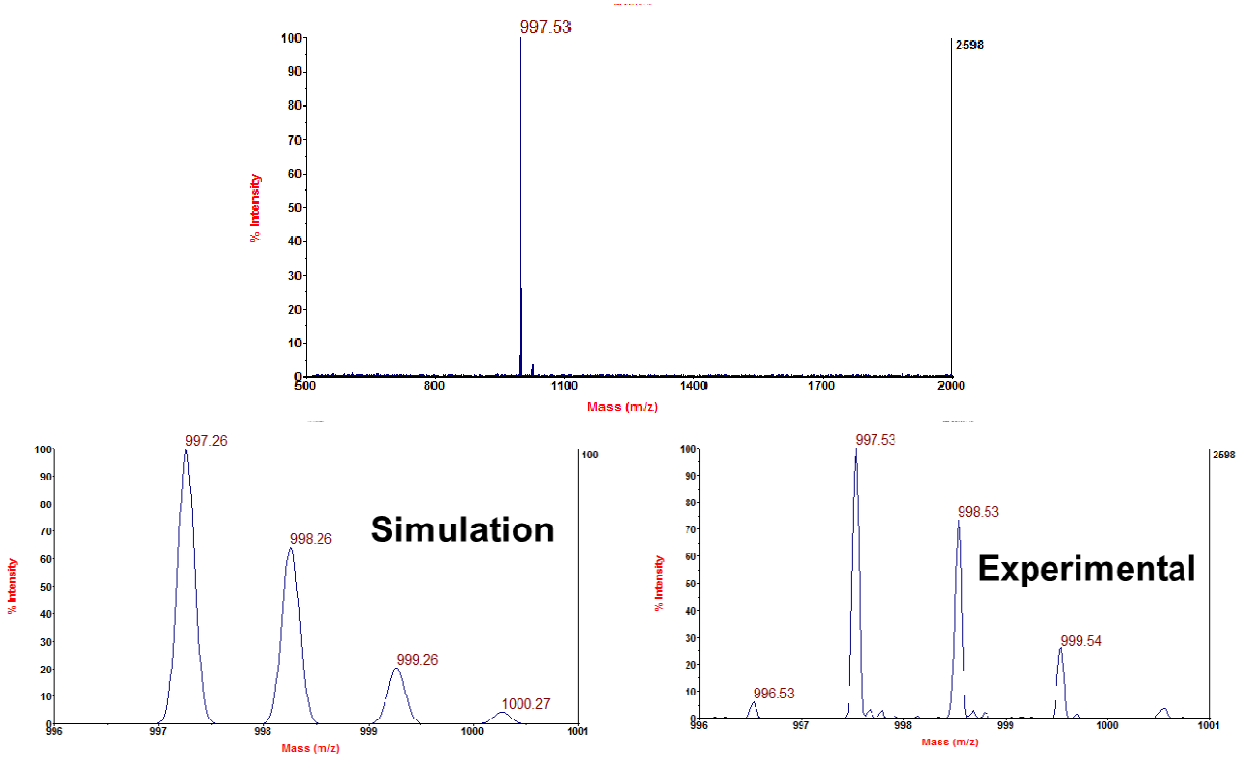

Figure S20. MALDI-TOF spectrum (positive mode, 1,4-diphenylbutadiene as matrix) of porphyrin **7** (top and bottom right) and corresponding isotope simulation (bottom left) expected for $C_{55}H_{33}F_{10}N_7O$.

Synthesis of 5,10,15-*tris*(3,5-di-*tert*-butylphenyl)-20-(4-carbomethoxyphenyl)-7,8,17,18-tetrabromoporphyrin **8**:

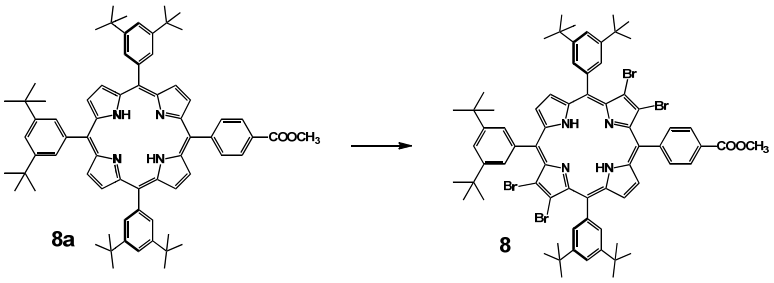

Note: Commercial N-bromosuccinimide (NBS) was freshly recrystallized from hot water, filtered through paper and dried under vacuum prior to use (white solid). In a round bottom flask, starting porphyrin **8a** (S3a) (0.116 g, 0.115 mmol) and fresh recrystallized NBS (0.133 g, 0.748 mmol) were dissolved in 50 mL of chloroform and the resulting purple solution was heated at reflux for 3 h. Another portion of NBS (0.041 g, 0.230 mmol) was added and the reaction mixture was stirred at reflux for additional 3 h, followed by a final addition of another portion of NBS (0.041 g, 0.230 mmol) and additional 3 h stirring at reflux. After cooling, water was added and the organic layer washed with water (3 × 100 mL), dried over $MgSO_4$, filtered through paper and concentrated. Final purification was achieved by column chromatography (SiO_2) using a gradient of hexanes/dichloromethane (from 90:10 to 40:60, v/v) to afford the target compound as a dark brownish purple solid in 32% yield (0.05 g, 0.037 mmol). ^{1}H NMR (400 MHz, $CDCl_3$, δ ppm): 8.82 (brs, 3H, pyrrolic protons); 8.64 (d, 1H, J = 5.0 Hz, pyrrolic proton); 8.45 (d, 2H, J = 8.3 Hz, H3”); 8.28 (d, 2H, J = 8.3 Hz, H2”); 7.99

(m, 6H, H2'); 7.83 (s, 3H, H4'); 4.10 (s, 3H, COOC<u>H</u>$_3$); 1.51 (s, 54H, Bu$_t$); -2.88 (s, 1H, N<u>H</u>); -2.91 (s, 1H, N<u>H</u>). MALDI-TOF (positive mode, 1,4-diphenylbutadiene as matrix) 1324.02 $(M)^+$, calculated 1324.3 for $C_{70}H_{76}N_4O_2Br_4$.

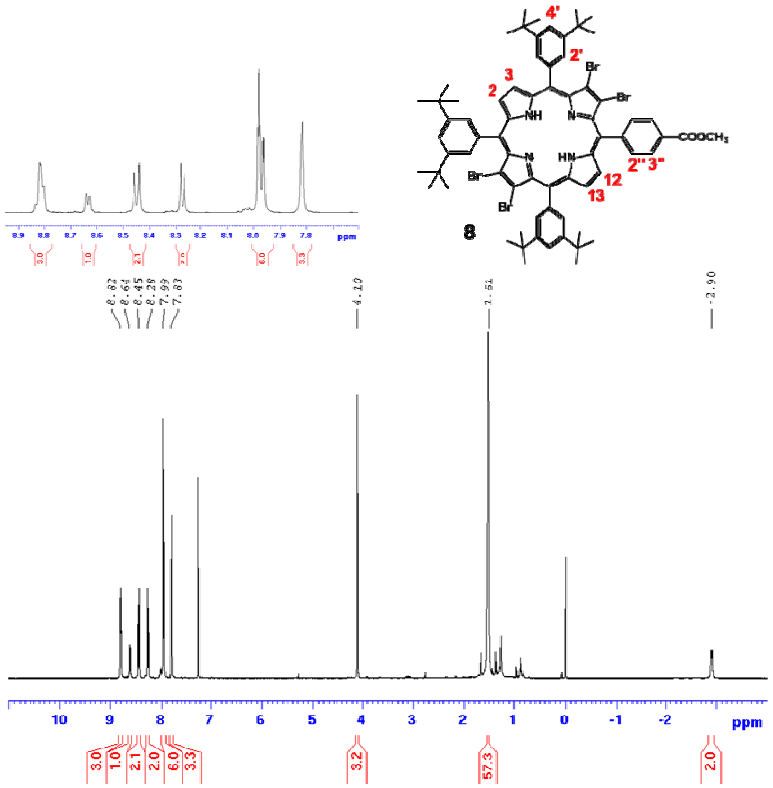

Figure S21. ^{1}H NMR spectrum of porphyrin **8**, 500 MHz, $CDCl_3$, 25^{o}C.

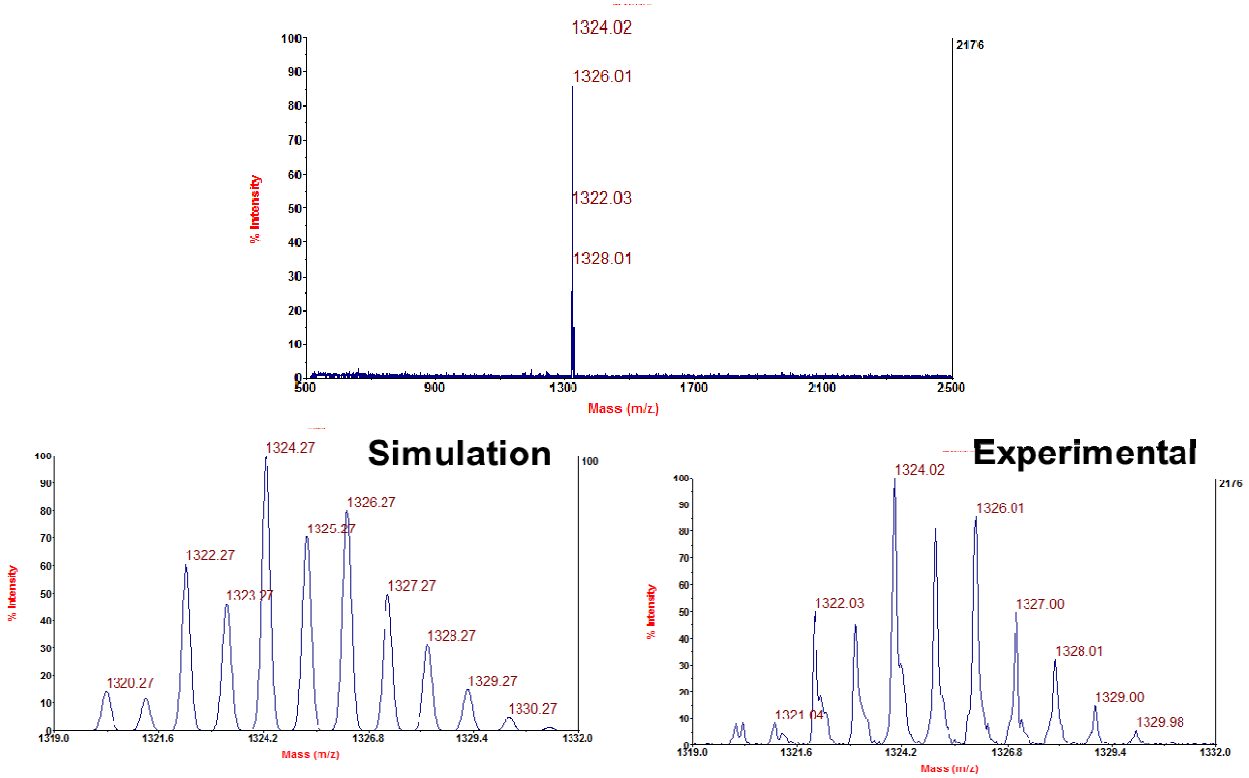

Figure S22. MALDI-TOF spectrum (positive mode, 1,4-diphenylbutadiene as matrix) of porphyrin **8** (top and bottom right) and corresponding isotope simulation (bottom left) expected for $C_{70}H_{76}N_4O_2Br_4$.

Synthesis of 5,10,15-*tris*(3,5-di-*tert*-butylphenyl)-20-(4-carbomethoxyphenyl)-7,8,17,18-tetracyanoporphyrin **9**:

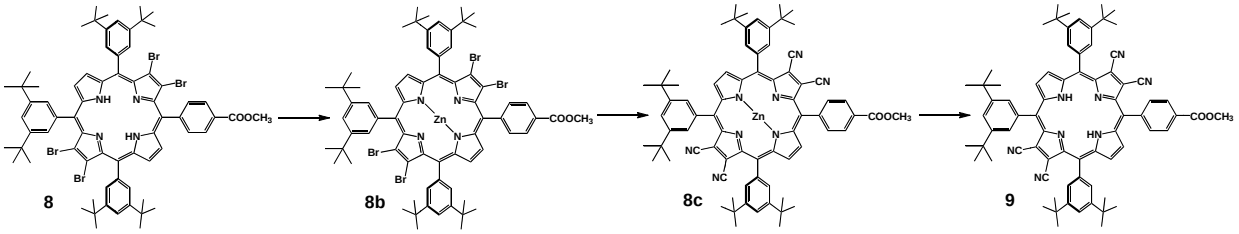

First step: Synthesis of porphyrin **8b**. Porphyrin **8** (0.05 g, 0.037 mmol) and $Zn(OAc)_2$ (0.083 g, 0.377 mmol) were dissolved in 100 mL of a mixture of chloroform/methanol (90:10, v/v) and the resulting purple solution was heated at reflux for 1 h. After cooling, water was added and the organic layer washed with water (3 × 100 mL), dried over $MgSO_4$, filtered through paper and concentrated. Final purification was achieved by flash chromatography (SiO_2) using dichloromethane as eluent to afford the target compound **8b** as a dark purple solid in quantitative yield (0.050 g, 0.037 mmol). ^{1}H NMR (400 MHz, $CDCl_3$, δ ppm): 8.87 (m, 2H, pyrrolic protons); 8.83 (d, 1H, J = 5 Hz, pyrrolic proton); 8.67 (d, 1H, J = 5 Hz, pyrrolic proton); 8.36 (d, 2H, J = 8.1 Hz, H3"); 8.15 (d, 2H, J = 8.1 Hz, H2"); 7.85 (s, 6H, H2'); 7.79 (s, 3H, H4'); 4.06 (s,

3H, COOC<u>H</u>$_3$); 1.51 (s, 54H, Bu$_t$). MALDI-TOF (positive mode, 1,4-diphenylbutadiene as matrix) 1388.56 $(M)^+$, calculated 1388.2 for $C_{70}H_{74}N_4O_2Br_4Zn$.

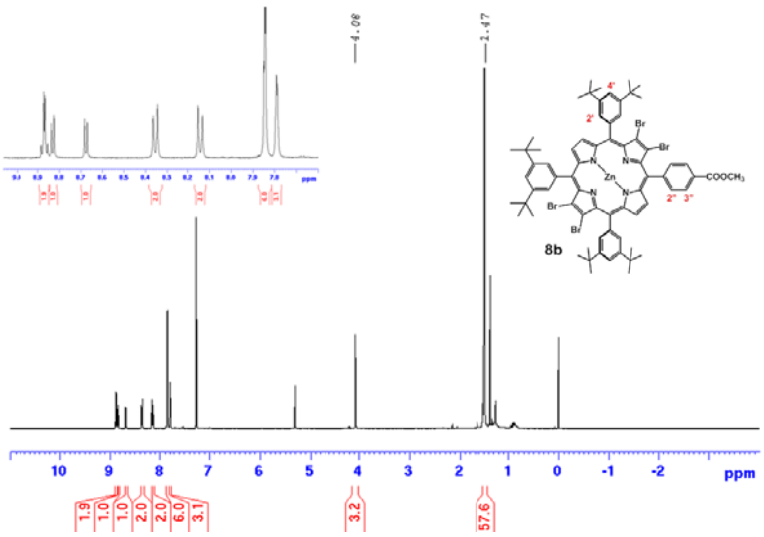

Figure S23. ^{1}H NMR spectrum of porphyrin intermediate **8b**, 400 MHz, $CDCl_3$, 25^{o}C.

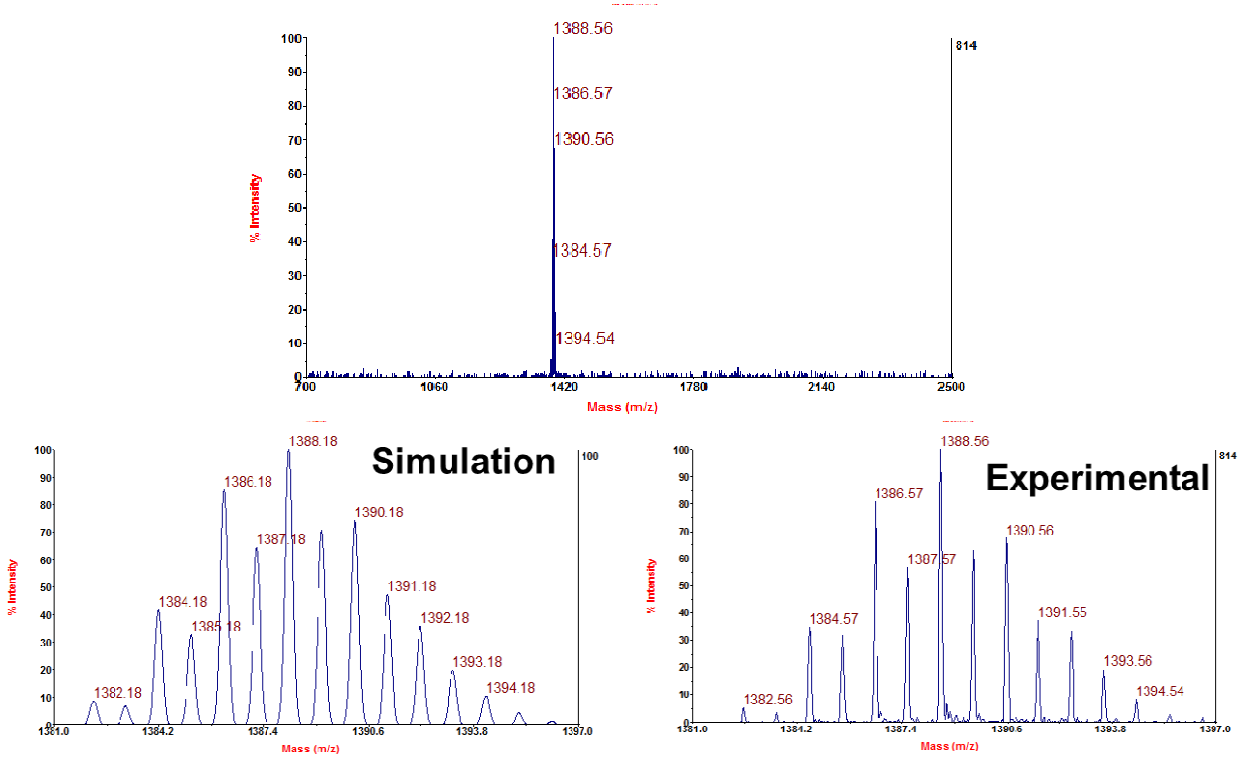

Figure S24. MALDI-TOF spectrum (positive mode, 1,4-diphenylbutadiene as matrix) of porphyrin **8b** (top and bottom right) and corresponding isotope simulation (bottom left) expected for $C_{70}H_{74}N_4O_2Br_4Zn$.

Second step: Synthesis of porphyrin **8c**. Porphyrin **8b** (0.034 g, 0.0245 mmol), $Zn(CN)_2$ (0.007 g, 0.058 mmol), [1,10-bis-(diphenylphosphino)ferrocene] (dppf) (0.022 g, 0.039 mmol), zinc dust (0.002 g, 0.03 mmol), zinc(II)acetate (0.002 g, 0.011 mmol) were all dissolved in 5 mL of anhydrous oxygen-free dimethylacetamide and stirred at room temperature for 2 min. Tris(dibenzylideneacetone)dipalladium(0) ($Pd_2(dba)_3$) (0.018 g, 0.019 mmol) was added and the reaction mixture was stirred at 100°C for 12 h under an inert atmosphere. After cooling, dichloromethane (50 mL) was added and the green organic phase was washed with water (2 × 50 mL), dried over sodium sulfate, filtered through paper and concentrated under reduced pressure. Final purification was achieved by column chromatography (SiO_2) using toluene/ethyl acetate (90:10) to afford porphyrin **8c** as a bluish green solid in 49% yield (0.014 g). ^{1}H NMR (400 MHz, $CDCl_3$, δ ppm): 8.87 (m, 3H, pyrrolic protons); 8.70 (d, 1H, pyrrolic protons); 8.39 (d, 2H, *J* = 8.0 Hz, H3"); 8.15 (d, 2H, *J* = 8.0 Hz, H2"); 7.94 (s, 3H, H4'); 7.67 (s, 6H, H2'); 4.06 (s, 3H, $COOCH_3$); 1.49 (s, 54H, Bu_t).

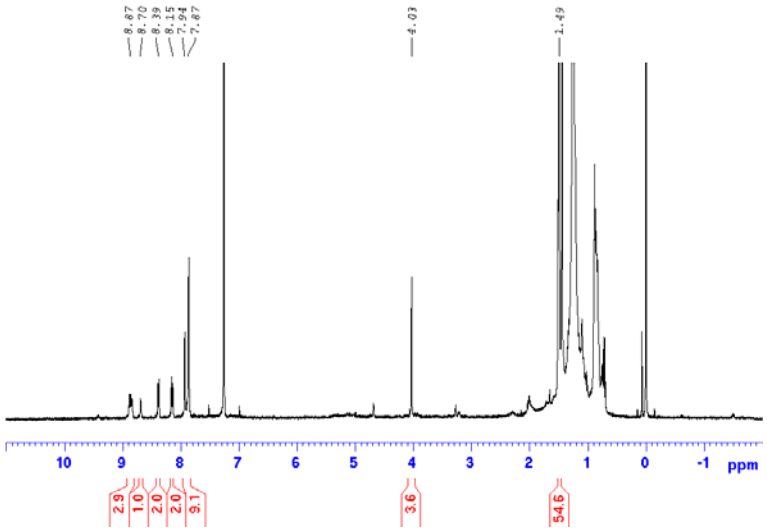

Figure S25. ^{1}H NMR spectrum of porphyrin intermediate **8c**, 400 MHz, $CDCl_3$, 25°C.

Third step: Synthesis of porphyrin **9**. Porphyrin **8c** (0.014 g, 0.012 mmol) was dissolved in 10 mL of dry dichloromethane and 10 mL of trifluoroacetic acid was added under an inert atmosphere. The brown reaction mixture was stirred for 30 min at room temperature. The crude product was neutralized with triethylamine, washed with water (2 × 10 mL), dried over sodium sulfate, filtered through paper and concentrated under reduced pressure. Final purification was achieved by flash chromatography (SiO_2) using dichloromethane as eluent to afford target porphyrin **9** as a bluish-green solid in 99% yield (0.013 g). ^{1}H NMR (400 MHz, $CDCl_3$, δ ppm): 9.01 (m, 3H, pyrrolic protons); 8.86 (dd, 1H, pyrrolic proton); 8.49 (d, 2H, *J* = 8.2 Hz, H3"); 8.26 (d, 2H, *J* = 8.2 Hz, H2"); 8.05-7.85 (m, 9H, H2' and H4'); 4.10 (s, 3H, $COOCH_3$); 1.53 (s, 54H, Bu_t); -2.43 (s, 1H, NH); -2.45 (s, 1H, NH).

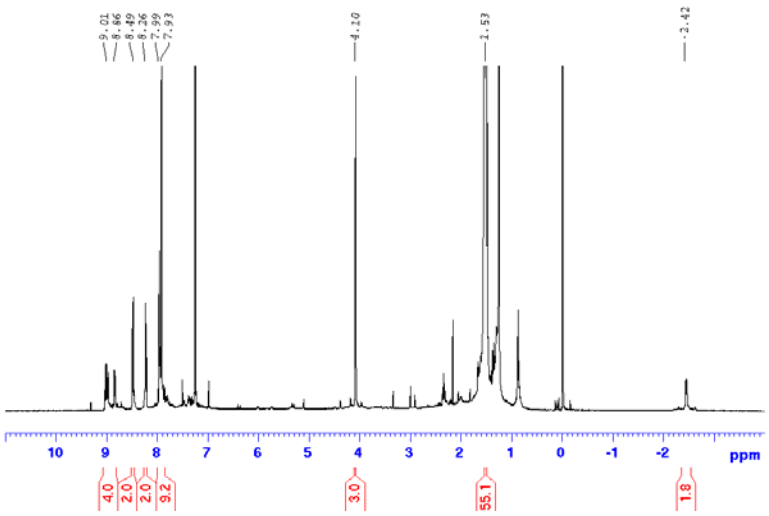

Figure S26. ^{1}H NMR spectrum of porphyrin intermediate **9**, 400 MHz, $CDCl_3$, 25^{o}C.

Synthesis of 5,10,15-*tris*(3,5-di-*tert*-butylphenyl)-20-(4-carboxyphenyl)-7,8,17,18-tetracyanoporphyrin **10**:

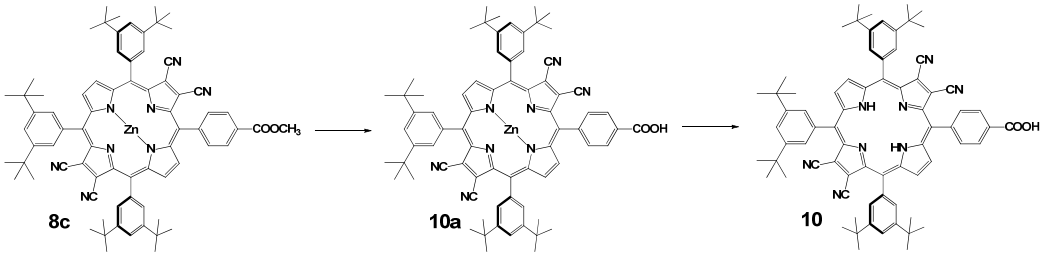

Porphyrin **8c** (0.014 g, 0.012 mmol) was dissolved in 5 mL of tetrahydrofuran followed by addition of a 10 % KOH aqueous solution (w/w) and the reaction mixture was stirred for 2 h at room temperature. After the reaction time, dichloromethane (30 mL) was added; the organic phase was copiously washed with water (3 × 100 mL), dried over sodium sulfate, filtered through paper and concentrated under reduced pressure at room temperature to about 10 mL. The green crude mixture containing **10a** was then treated with 10 mL of trifluoroacetic acid for 1 h at room temperature to remove the zinc ion from the porphyrin. The crude mixture was diluted with 20 mL of dichloromethane, neutralized with triethylamine, washed with water (3 × 50 mL), dried over sodium sulfate and concentrated under reduced pressure. Final purification was achieved by flash chromatography (SiO_2) using dichloromethane/methanol (9:1, v/v) as eluent to afford target porphyrin **10** as a bluish-green solid in 90% yield (0.011 g). MALDI-TOF (negative mode, 1,4-diphenylbutadiene as matrix) 1094.41 $(M)^{-}$, calculated 1094.6 for $C_{73}H_{74}N_8O_2$.

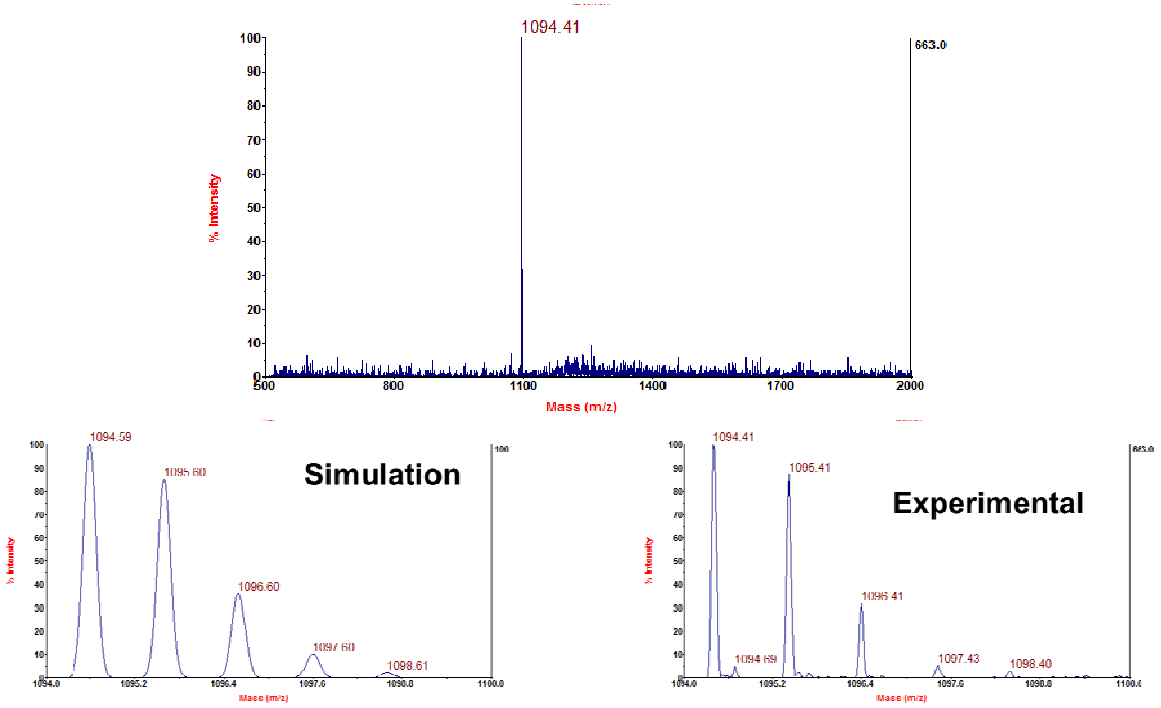

Figure S27. MALDI-TOF spectrum (negative mode, 1,4-diphenylbutadiene as matrix) of porphyrin **10** (top and bottom right) and corresponding isotope simulation (bottom left) expected for $C_{73}H_{74}N_8O_2$.

Synthesis of 5,15-bis(2,3,4,5,6-pentafluorophenyl)-10-(4-nitrophenyl)-20-(3-formyl-4-hydroxy-5-*tert*-butylpheynyl)zinc(II)porphyrin **2a**

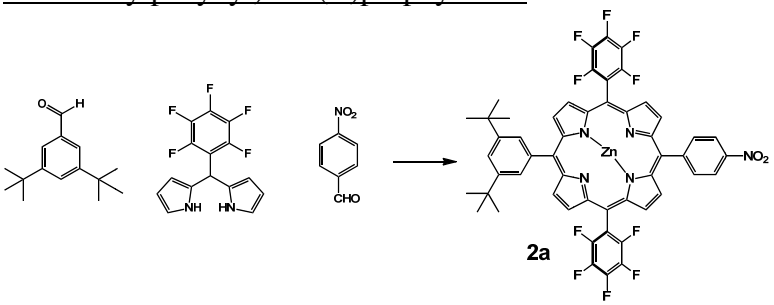

Commercially-available 3,5-di-*tert*-butylbenzaldehyde (0.401 g, 1.84 mmol), 4-nitrobenzaldehyde (0.278 g, 1.84 mmol) and pentafluorophenyl-dipyrromethane (1.15 g, 3.68 mmol) were dissolved in 370 mL of chloroform containing 2.45 mL (0.75 %, v/v) of ethanol under a nitrogen atmosphere, followed by addition of boron-trifluoride etherate (BF_3OEt_2) (0.065 g, 0.065 mL, 0.46 mmol) and the reaction mixture was stirred for one hour at room temperature. The resulting dark red porphyrogenic mixture was oxidized with 2,3-dichloro-5,6-dicyano-1,4-benzoquinone (DDQ) (1.25 g, 5.50 mmol) for 12 h at room temperature, yielding a black crude mixture. Filtration through a silica pad to remove tar and polymeric byproducts, followed by concentration under reduced pressure afforded a reddish purple solid, which was dissolved in dichloromethane (100 mL) followed by addition of $Zn(OAc)_2$ (1.10 g, 5 mmol) dissolved in 20 mL of methanol. The purple solution was heated at reflux for 1 h. After cooling, water was added, the organic layer separated and washed with water (3 × 100 mL), dried over $MgSO_4$, filtered through paper and concentrated. Final purification was achieved by flash chromatography (SiO_2) using dichloromethane as eluent to afford the target compound **2a** as a

dark purple solid in 10% yield (0.372 g). ^{1}H NMR (400 MHz, $CDCl_3$, δ ppm): 9.15 (d, 2H, pyrrolic protons); 8.95 (m, 6H, pyrrolic protons); 8.64 (d, 2H,*J* = 8.2 Hz, H3"); 8.42 (d, 2H, *J* = 8.2 Hz, H2"); 8.07 (s, 2H, H2'); 7.87 (s, 1H, H4'); 1.57 (s, 18H, Bu_t). MALDI-TOF (positive mode, 1,4-diphenylbutadiene as matrix) 1013.30 $(M)^+$, calculated 1013.20 for $C_{52}H_{33}F_{10}N_5O_2Zn$.

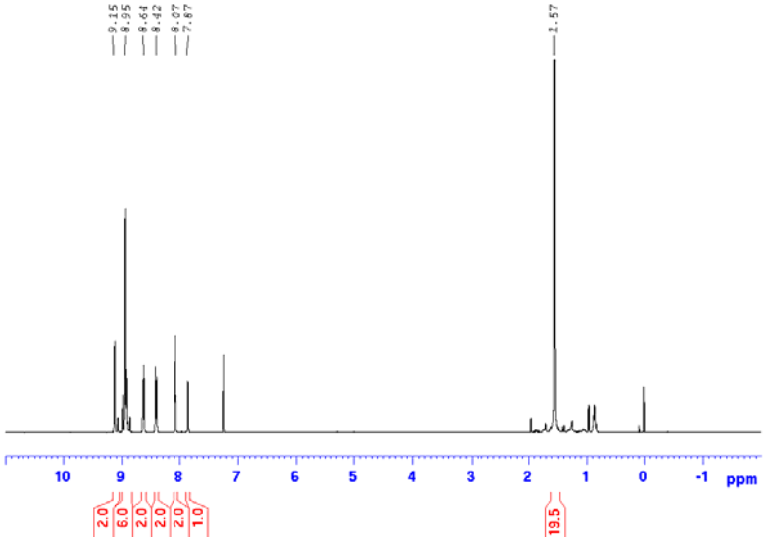

Figure S28. ^{1}H NMR spectrum of porphyrin intermediate **2a**, 400 MHz, $CDCl_3$, 25°C.

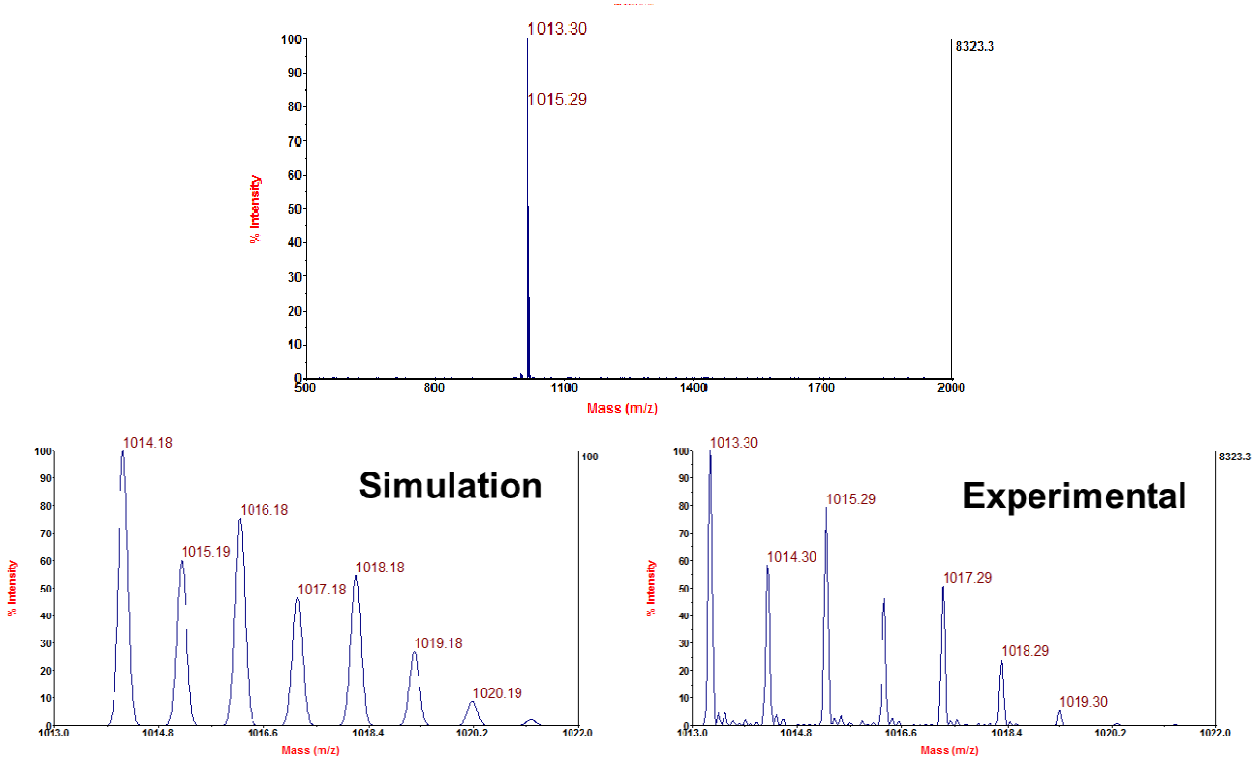

Figure S29. MALDI-TOF spectrum (positive mode, 1,4-diphenylbutadiene as matrix) of porphyrin **2a** (top and bottom right) and corresponding isotope simulation (bottom left) expected for $C_{52}H_{33}F_{10}N_5O_2Zn$.

Synthesis of 5,15-bis(2,3,4,5,6-pentafluorophenyl)-10-(4-aminophenyl)-20-(3-formyl-4-hydroxy-5-*tert*-butylpheynyl)porphyrin **2b**

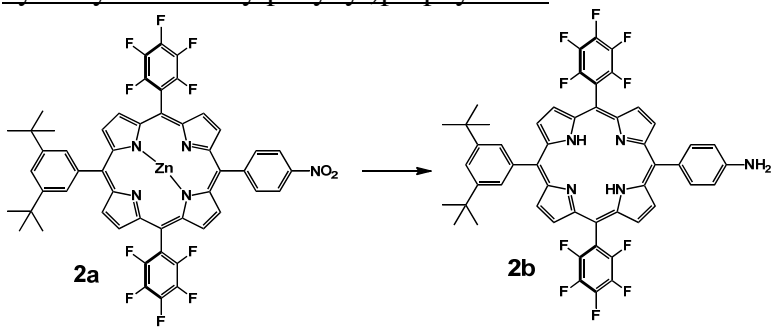

Porphyrin **2a** (0.103 g, 0.1 mmol), 10% palladium on carbon (0.10 g) and $NaBH_4$ (0.019 g, 0.5 mmol) were suspended in 40 mL of a mixture of dichloromethane and methanol (1:1). The suspension was stirred at room temperature for 5 h under nitrogen atmosphere before filtering the reaction mixture through a pad of Celite. The solvent was evaporated under reduced pressure and the crude was re-dissolved in dichloromethane 20 mL, washed with water (3 × 50 mL), dried over $MgSO_4$ and filtered through paper. The organic phase was then treated with 20 mL of trifluoroacetic acid for 1 h at room temperature. The solution was neutralized with triethylamine, washed with water (3 × 50 mL), dried over $MgSO_4$, filtered through paper and concentrated. Final purification was achieved by column chromatography (SiO_2) using a gradient of hexanes/dichloromethane (from 90:10 to 50:50, v/v) as eluent to afford the target compound as a purple solid in 65% yield (0.06 g, 0.065 mmol). ^{1}H NMR (400 MHz, $CDCl_3$, δ ppm): 9.07 (d, 2H, *J* = 7 Hz, pyrrolic protons); 8.96 (d, 2H, *J* = 7 Hz, pyrrolic protons); 8.79 (d, 4H, *J* = 7 Hz, pyrrolic protons); 8.06 (s, 2H, H2'); 7.99 (d, 2H, *J* = 8.5 Hz, H2"); 7.84 (s, 1H, H4'); 7.07 (d, 2H, *J* = 8.5 Hz, H3"); 4.03 (s, 2H, NH_2); 1.54 (s, 18H, Bu_t); -2.78 (s, 2H, NH). MALDI-TOF (positive mode, 1,4-diphenylbutadiene as matrix) 921.38 $(M)^+$, calculated 921.3 for $C_{52}H_{37}F_{10}N_5$.

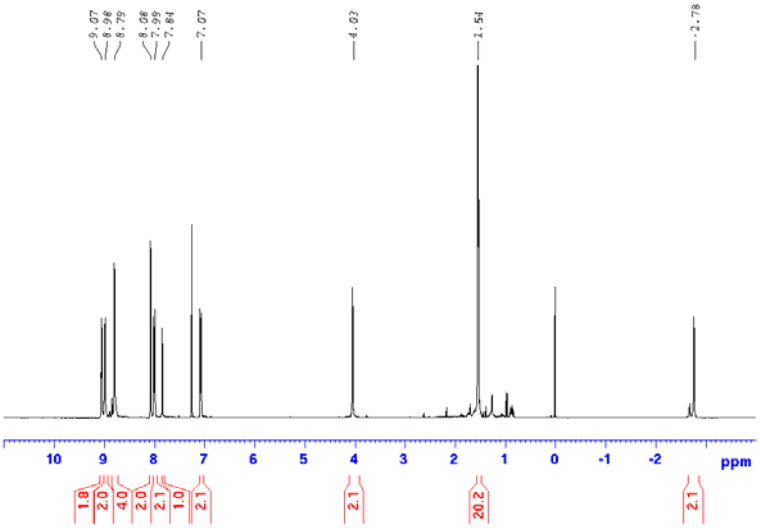

Figure S30. ^{1}H NMR spectrum of porphyrin intermediate **2**, 400 MHz, $CDCl_3$, 25°C.

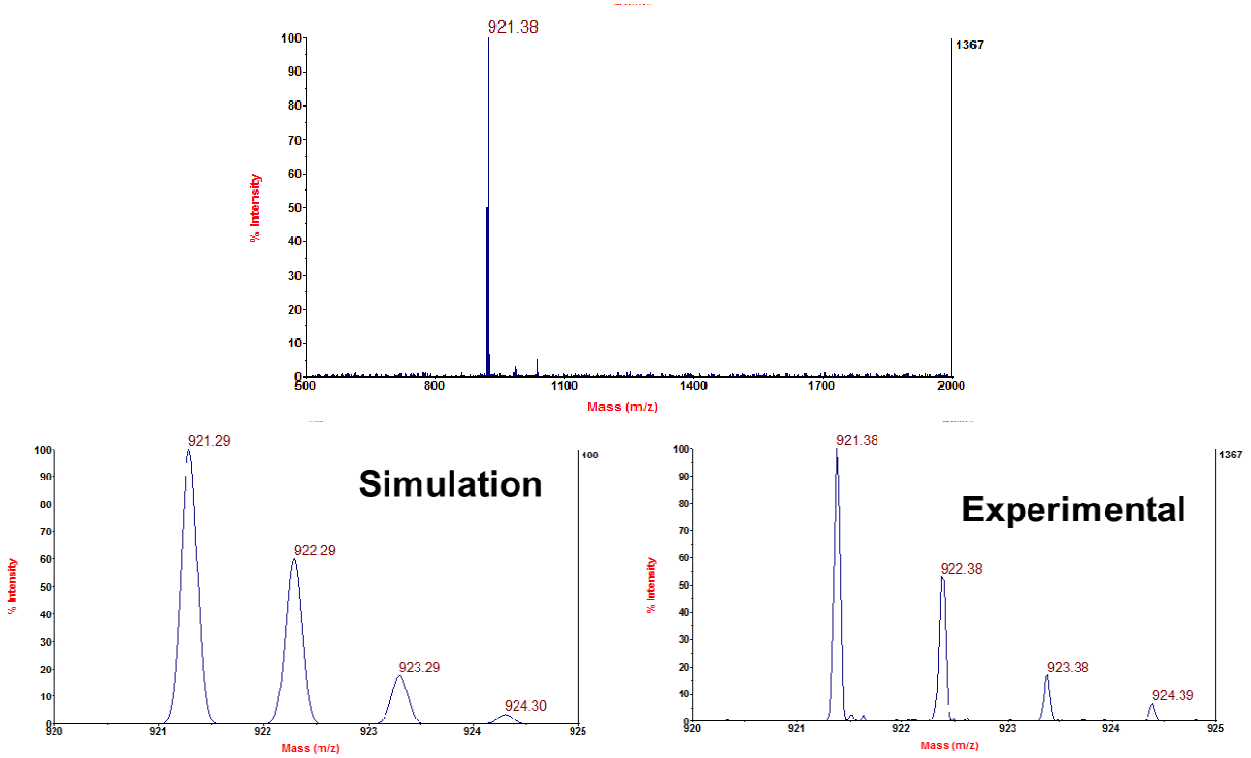

Figure S31. MALDI-TOF spectrum (positive mode, 1,4-diphenylbutadiene as matrix) of porphyrin **2b** (top and bottom right) and corresponding isotope simulation (bottom left) expected for $C_{52}H_{37}F_{10}N_5$.

3.4 – Synthesis and Spectroscopic Characterization of Dyad 2.

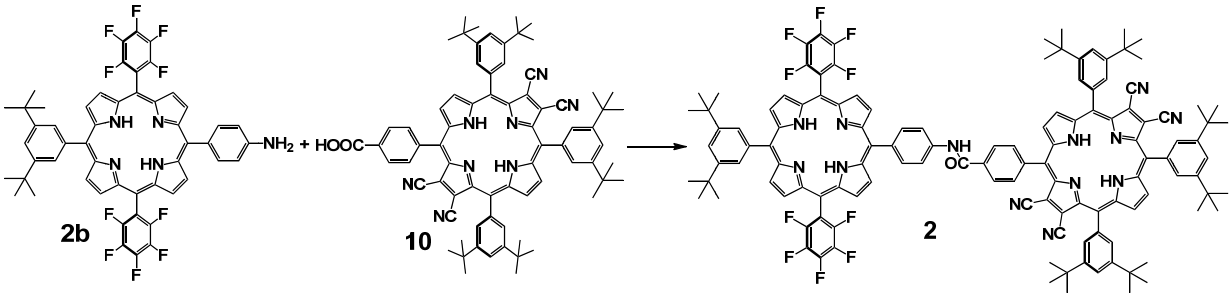

Porphyrins **2b** (0.0055 g, 6.00 µmol) and **10** (0.006 g, 5.48 µmol) were dissolved in 3 mL of dichloromethane under inert atmosphere. Dimethylaminopyridine (DMAP) (0.002 g, 0.01mmol) and 1-ethyl-3-(3-dimethylaminopropyl)carbodiimide (0.002 g, 8.22 µmol) were added and the reaction mixture was stirred at room temperature for 12 h. The crude mixture was diluted with 20 mL of dichloromethane, washed with water (3 × 20 mL), dried over $MgSO_4$, filtered through paper and concentrated. Final purification was achieved by column chromatography (SiO_2) using a gradient of hexanes/dichloromethane as eluent to afford the target compound as a greenish-purple solid in 56% yield (0.007 g, 3.33 µmol). ^{1}H NMR (400 MHz, $CDCl_3$, δ ppm): 9.06 (m, 4H, pyrrolic protons); 9.00 (m, 4H, pyrrolic protons); 8.85 (d, 2H, *J* = 5.0 Hz, pyrrolic protons); 8.81 (d, 2H, *J* = 5.0 Hz, pyrrolic protons); 8.70 (s, 1H, NHCO); 8.44 (d, 2H, *J* = 8.3 Hz, H2”); 8.39 (d, 2H, *J* = 8.3 Hz, H3”); 8.33 (d, 2H, *J* = 8.4 Hz, H2’); 8.25 (d, 2H, *J* = 8.4 Hz, H3’); 8.08

(s, 3H, Hp'); 8.03-7.90 (m, 7H, Hp and Ho'); 7.84 (s, 2H, Ho); 1.54 (m, 72H, Bu_t); -2.38 (s, 2H, NH); -2.79 (s, 2H, NH). MALDI-TOF (positive mode, 1,4-diphenylbutadiene as matrix) 1999.53 $(M)^+$, calculated 1997.9 for $C_{125}H_{109}F_{10}N_{13}O$.

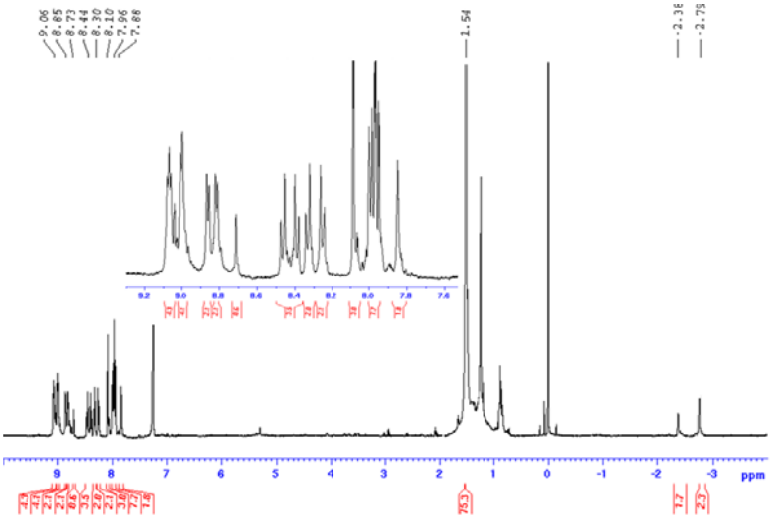

Figure S32. ^{1}H NMR spectrum of dyad **2**, 400 MHz, $CDCl_3$, 25°C.

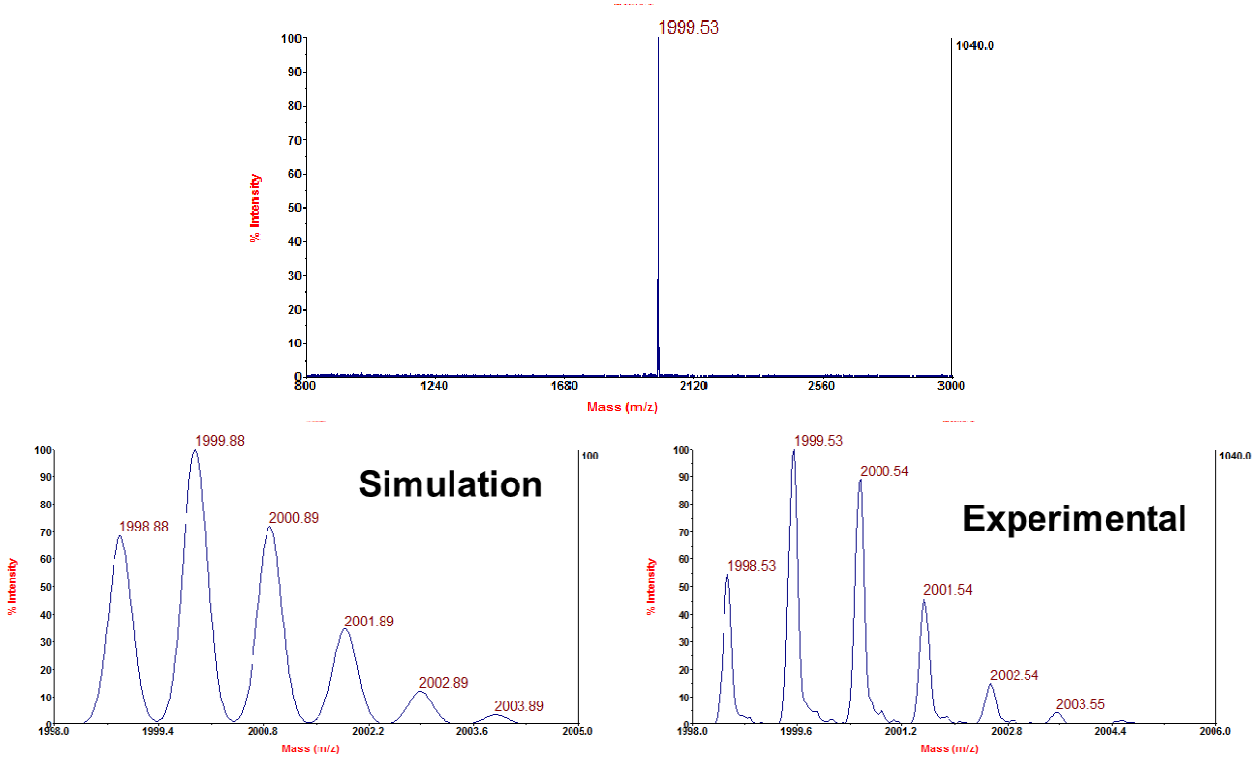

Figure S33. MALDI-TOF spectrum (positive mode, 1,4-diphenylbutadiene as matrix) of dyad **2** (top and bottom right) and corresponding isotope simulation (bottom left) expected for $C_{125}H_{109}F_{10}N_{13}O$.

3.5 – Synthesis and Spectroscopic Characterization of Triad 1.

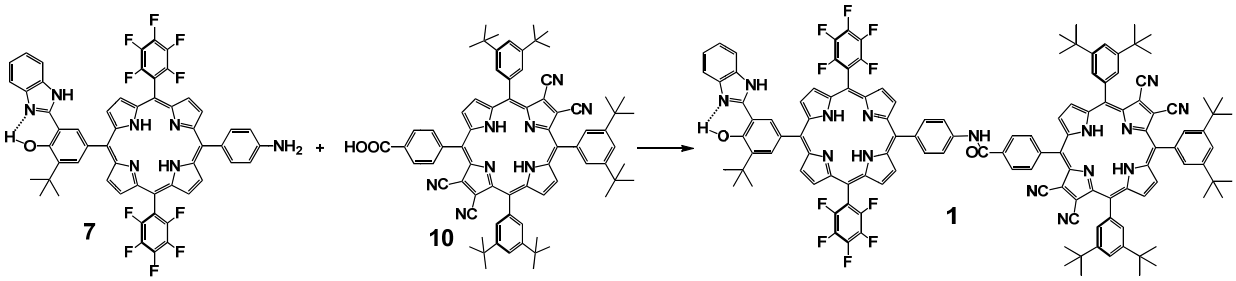

Porphyrins **7** (0.006 g, 6.00 μmol) and **10** (0.006 g, 5.48 μmol) were dissolved in 3 mL of dichloromethane under inert atmosphere. Dimethylaminopyridine (DMAP) (0.002 g, 0.01mmol) and 1-ethyl-3-(3-dimethylaminopropyl)carbodiimide (0.002 g, 8.22 μmol) were added and the reaction mixture was stirred at room temperature for 12 h. The crude mixture was diluted with 20 mL of dichloromethane, washed with water (3 × 20 mL), dried over $MgSO_4$, filtered through paper and concentrated. Final purification was achieved by column chromatography (SiO_2) using a gradient of hexanes/dichloromethane as eluent to afford the target compound as a greenish-purple solid in 59% yield (0.0067 g, 3.32 μmol). MALDI-TOF (positive mode, 1,4-diphenylbutadiene as matrix) 2074.69 $(M + H)^+$, calculated 2073.8 for $C_{128}H_{105}F_{10}N_{15}O_2$.

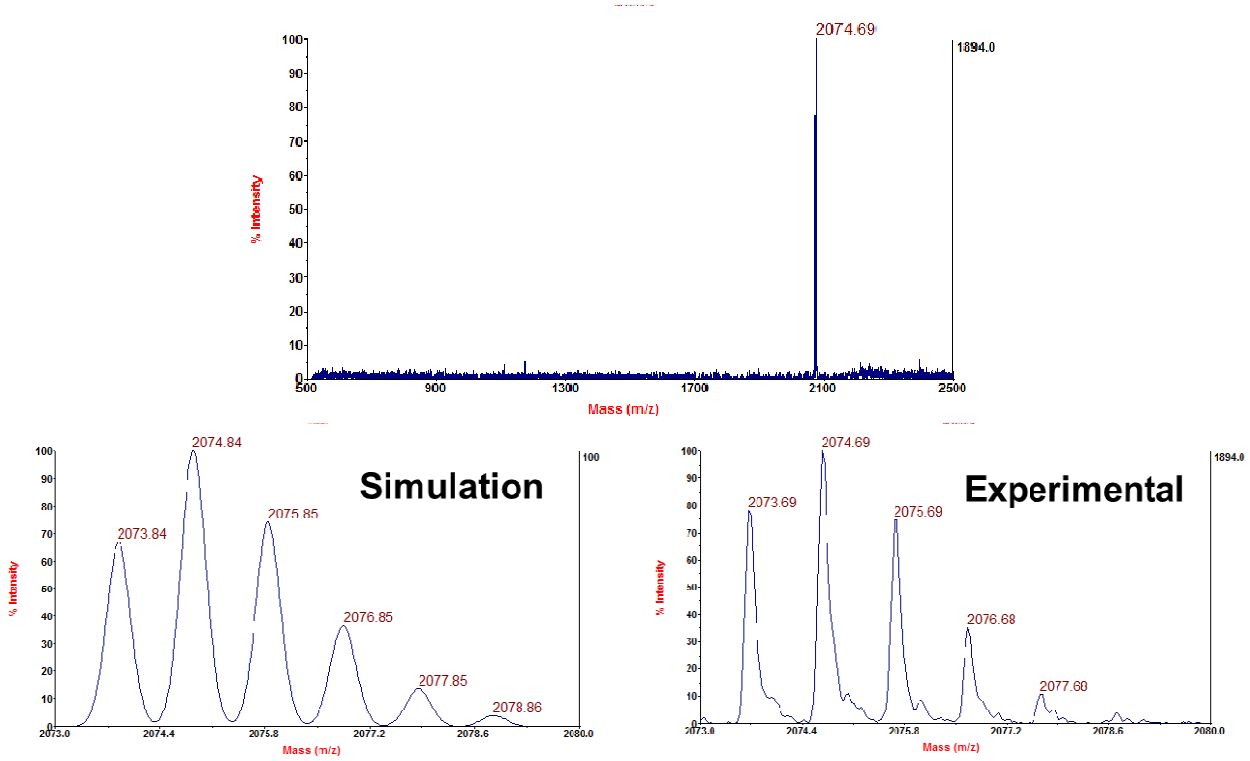

Figure S34. MALDI-TOF spectrum (positive mode, 1,4-diphenylbutadiene as matrix) of triad **1** (top and bottom right) and corresponding isotope simulation (bottom left) expected for $C_{128}H_{105}F_{10}N_5O_2$.

3.6 – References

S2 – Jacobsen, J.F.L *et al.* Journal of Organic Chemistry, 1994, **59**, p. 1939-1942.

S3 – a) Lindsey, J.S. Accounts of Chemical Research, 2010, **43**, 300–311. b) Gary F. Moore, M.H. Miguel Gervaldo, Oleg G. Poluektov, Tijana Rajh, Devens Gust, Thomas A. Moore and Ana L. Moore. Journal of the American Chemical Society, 2008, **130**, 10466–10467.